ESTIMATION OF THE SOLAR RADIATION FLUX FOR AN ARCTIC SURFACE

ESTIMATION OF THE SOLAR RADIATION FLUX FOR AN ARCTIC SURFACE

by

WILLIAM KIM CARLETON WHITE

A Research Paper
Submitted to the Department of Geography
in Fulfillment of the Requirements
for
Geography 4B6

McMaster University
September 1978

ABSTRACT

A previous study (Davies and Hay, 1978) described a method of calculating hourly and daily values of global solar radiation for cloudless and cloudy sky conditions. This scheme, requiring only upper air data from daily radiosonde ascents, and hourly surface weather observations, has been used successfully at a number of mid latitude sites (Davies et al., 1975; Suckling and Hay, 1976). In this investigation the extention of this method for use in an Arctic environment is presented.

Solar radiation received at the earth's surface is the sum of direct and diffuse components. The flux in cloudless conditions is calculated as the residual after attenuation of solar irradiance by water vapour, ozone, Rayleigh scattering and aerosol. Cloudless sky values are then adjusted for cloud effects, using a cloud layer method similar to that used by Davies et al. in Southern Ontario, Canada.

The computed values are compared with values measured at Resolute, N.W.T., Canada. Under cloudless sky conditions hourly and daily calculated values agree well with measurements. For days of cloud amount less than 4/10, model overestimates are observed. As cloud amounts increase varying degrees of model underestimation of measured values occur. This is linked with observer inability to adequately specify cloud amount, and the variation of cloud type transmission characteristics for Arctic areas.

ACKNOWLEDGEMENTS

I would like to express my sincere appreciation for the assistance, patience and supervision of Dr. J.A. Davies, without whose invaluable guidance this study would not have been possible. To Dr. W. Rouse a note of thanks for his encouragement throughout the years. A special thanks goes to Mr. A. Sawchuck who was instrumental in editing this text. Also, I would like to thank Mr. P. Mills for computer assistance and Mrs. C. Moulder for manuscript preparation.

TABLE OF CONTENTS

LIST OF ILLUSTRATIONS

LIST OF TABLES

CHAPTER 1

INTRODUCTION

The geographical distribution of global solar radiation received at the earth's surface, is an important parameter in determining the distribution and magnitude of most energy driven processes. For Canada, meteorological stations measuring this flux are sparcely distributed, especially in the Arctic as is shown in Figure 1. This condition serves to limit data availability, which could prove beneficial to such diverse fields as climatology, meteorology, glaciology, hydrology andecology.

In the absence of direct measurement, the need arises for procedures to calculate solar flux densities. However, satisfactory schemes are few and those undertaken for Arctic areas, generally concern themselves with the spatial distribution of global solar radiation. Although useful for macro-scale investigations values for shorter periods, perferably daily, would have wider application.

For daily values solar radiation computational schemes must include parameters to account for astronomical, geographical and atmospheric processes. However, the necessity also exists for schemes which utilize readily available meteorological data. These requirements may be met through the use of the physically-based approach outlined by Davies and Hay, 1978. Although simple, requiring only hourly cloud observations, and precipitable water, this type of model has been used successfully at a number of mid-latitude sites (Davies, Schertzer and Nunez, 1975; Suckling and Hay, 1977). These workers have succeeded in inferring the models applicability for locations, where hourly meteorological data (including cloud observations are available (Table 1, Figure 1) is available . Still little is known about its application to Arctic areas.

Table I : Comparison of Canadian stations measuring total solar radiation and those where hourly meterological (including clouds obs.) data are available, as of January 1, 1976. (after Suckling and Hay, 1977)

Region	Number of stations for		Total	Fractional Increase
	Measuring	Modelling		
East Coast Provinces	7	17	24	3.4
Quebec	6	11	17	2.8
Ontario	6	13	19	3.2
Prairie Provinces	8	23	31	3.9
British Columbia	9	14	23	2.6
The North	15	5	20	1.3
Canada (excl. North)	36	78	114	3.2
Canada	51	83	134	2.6

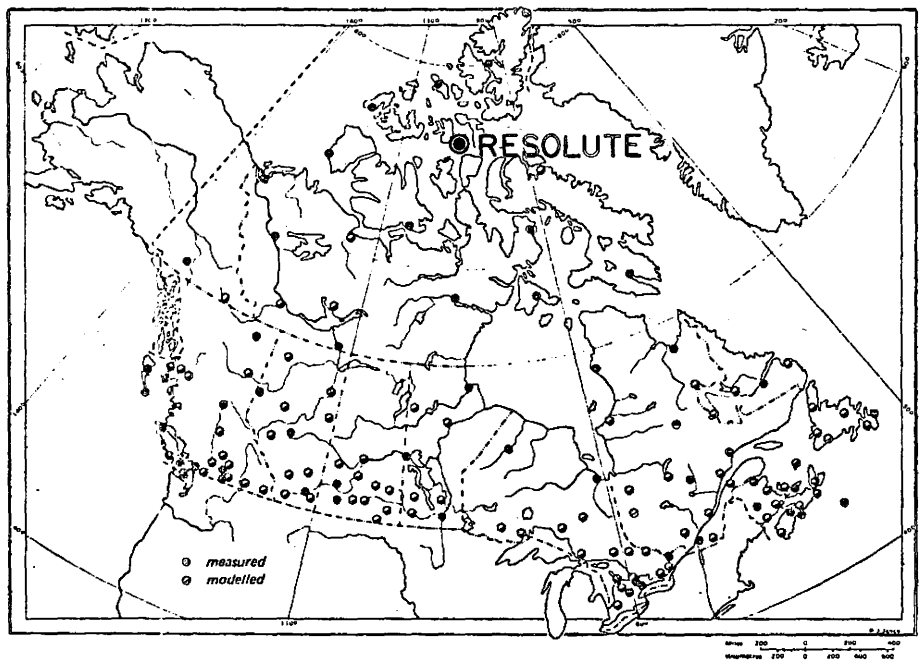

Figure I : Available solar radiation network in Canada, as of January 1, 1976:

- Stations measuring solar radiation
- Stations for potential modelling of solar radiation.

(after Suckling and Hay, 1977)

This thesis describes the results of a climatological investigation directed towards the application of the Davies and Hay (1978) approach for computing incoming solar flux density at the Atmosperic Environment Service first class station located at Resolute, N.W.T. ($74^{o}43'N$, $94^{o}59'W$) for the period April 1 through to August 31, 1974.

CHAPTER 2

PHYSICAL BASIS

(A) INTRODUCTION

In this chapter, the Layer Model and underlying theory are presented. Cloudless-sky solar radiation will be discussed first and then, the effects of cloud. This commonly used procedure (Houghton, 1954; Monteith, 1962; Lettau and Lettau, 1969; Hay, 1970; Atwater and Brown, 1974; Davies, Schertzer and Nunez, 1975; Davies and Idso, 1978) presupposes other atmospheric properties are not significantly changed by the presence of cloud.

(B) CLOUDLESS SKY THEORETICAL FRAMEWORK

For a cloudless atmosphere, solar radiation received at the surface is the residual flux, after atmospheric absorption and scattering has depleted the extraterrestrial intensity. Assuming negligable atmospheric emission, atmospheric attenuation for solar radiation is expressed by the radiative transfer equation. Following Kondrat'yev (1969) this can be stated as

$$\cos\theta \frac{dI_\lambda}{d\tau} = \frac{\sigma_\lambda}{4\pi(K_\lambda + \sigma_\lambda)} \int_{W=4\pi} I_\lambda(z,r')\ \gamma_\lambda(z,r',r)dW - I_\lambda(z,r)$$

where I_λ is the monochromatic radient intensity at wavelength λ ; θ is the angle between the direction of propagation and the normal to the surface; or zenith angle; $\gamma(z,r',r)$ is the phase function describing the angular distribution of scattered light from a particle; r' is the direction of the impinging rays; r is the direction taken by the rays after scattering; σ_λ is a mass scattering co-efficient; K_λ is a mass absorption co-efficient; W is the solid angle in the co-ordinate system; and τ is the optical depth

as given by $\tau = \int_0^{ZT} \zeta (K\lambda + \sigma_\lambda) dz$ where ζ is the air density.

For practical applications it is customary to simplify this equation by calculating direct and diffuse flux components seperately.

(C) DIRECT BEAM SOLAR RADIATION

For direct beam radiation the scattering phase function can be omitted. Integrating over the path length between the surface and the top of the atmosphere, Z_T, equation 1 reduces to Beer's Law:

$$I = I\ (Z_T) \exp(-m\ \tau_\lambda) \qquad (2)$$
$$= I_\lambda\ (\psi_\lambda),$$

where m is the optical air mass ($m=\sec\theta$); τ_λ is the total optical depth for monochromatic radiation; and ψ_λ is the monochromatic transmittance for direct beam radiation.

The total optical depth is the sum of extinctions due to scattering and absorption processes. Thus

$$I_\lambda = I_\lambda(Z_T) \exp\left[-m(\tau_{O\lambda} + \tau_{W\lambda} + \tau_{R\lambda} + \tau_{a\lambda})\right] \qquad (3)$$

where $\tau_{O\lambda}$, $\tau_{W\lambda}$, $\tau_{R\lambda}$ and $\tau_{a\lambda}$ are respectively, the component optical depths due to absorption by ozone, water vapour, Rayleigh scattering, and extinction (absorption and scattering) by aerosols.

Alternatively equation (3) can be re-expressed by

$$I\lambda = I\lambda(Z_T) \cos\theta \cdot \psi_{O\lambda} \cdot \psi_{W\lambda} \cdot \psi_{R\lambda} \cdot \psi_{a\lambda} \qquad (4)$$

where $\psi_{O\lambda}$, $\psi_{W\lambda}$, $\psi_{R\lambda}$ and $\psi_{a\lambda}$ are the atmospheric transmittance due to

absorption by ozone, water vapour, Rayleigh scattering and extinction by aerosols.

Theoretically Beer's Law of exponential extinction is not applicable to broad spectral bands. For practical application it is forced to apply to the integrated spectrum. Since absorption due to water vapour $a_{w\lambda}$ occurs at wavelengths not affecting ozone or Rayleigh extinction; its absorptance should be subtracted (Atwater and Brown, 1974; Paltridge and Plat, 1976). Then, the direct beam radiation received at the surface is

$$I = I(Z_T) \cos\theta [(\psi_O \cdot \psi_R - aW)] \psi_a \qquad (5)$$

(D) DIFFUSE BEAM SOLAR RADIATION

The diffuse flux received at the surface is calculated by the procedure described by Davies and Hay (1978). The scattered portion of direct beam radiation reaching the surface consists of two components: one from Rayleigh scattering (D_R) and one from aerosol scattering (D_A). Assuming half of Rayleigh scattered radiation reaches the surface, and that water vapour only attenuates the direct beam (Paltridge, 1972), the downward component of Rayleigh scattering is

$$D_R = I_{(ZT)} \cos\theta \frac{\psi_O (1-\psi_R)\psi_a}{2} \qquad (6)$$

The diffuse component due to aerosol scattering is calculated by

$$D_A = I_{(ZT)} \cos\theta [\psi_O \cdot \psi_R - aW][1-\psi_a] W_O B_a \qquad (7)$$

where B_a is the ratio of forward to total scattering by aerosol, and W_o is a single scattering albedo representing the ratio of scattering to total

extinction, (absorption plus scattering).

Rosol and Schneider (1971) have demonstrated the need to incorporate secondary effects, arising from multiple reflections between the surface and the atmosphere. If α_g and α_R are the surface albedo and atmospheric albedo for surface reflected radiation the diffuse component arising from multiple reflection D_s is

$$D_s = \alpha_g \alpha_R \frac{(I + D_R + D_A)}{1 - \alpha_g \alpha_R} \tag{8}$$

The total diffuse flux density $D\downarrow$ is the sum of three components

$$D\downarrow = D_R + D_A + D_s \tag{9}$$

and the global solar radiation $K\downarrow_o$ under cloudless sky radiation is

$$K\downarrow_o = I + D\downarrow \tag{10}$$

Equation 10 is schematically shown in Figure 2 and 2A.

(E) CLOUDY SKY SOLAR RADIATION

Clouds modify the cloudless sky flux by attenuation, mainly due to scattering and by an enhancement due to multiple reflections between the ground and cloud. To allow for these effects a simple scheme based on Davies et al. (1975) is used. This procedure first calculates extinction by individual cloud layers, and then incorporates multiple reflection effects.

Assuming uniform cloud distribution for a cloud layer i, the cloud layer transmission Ψ_{ci} is defined by,

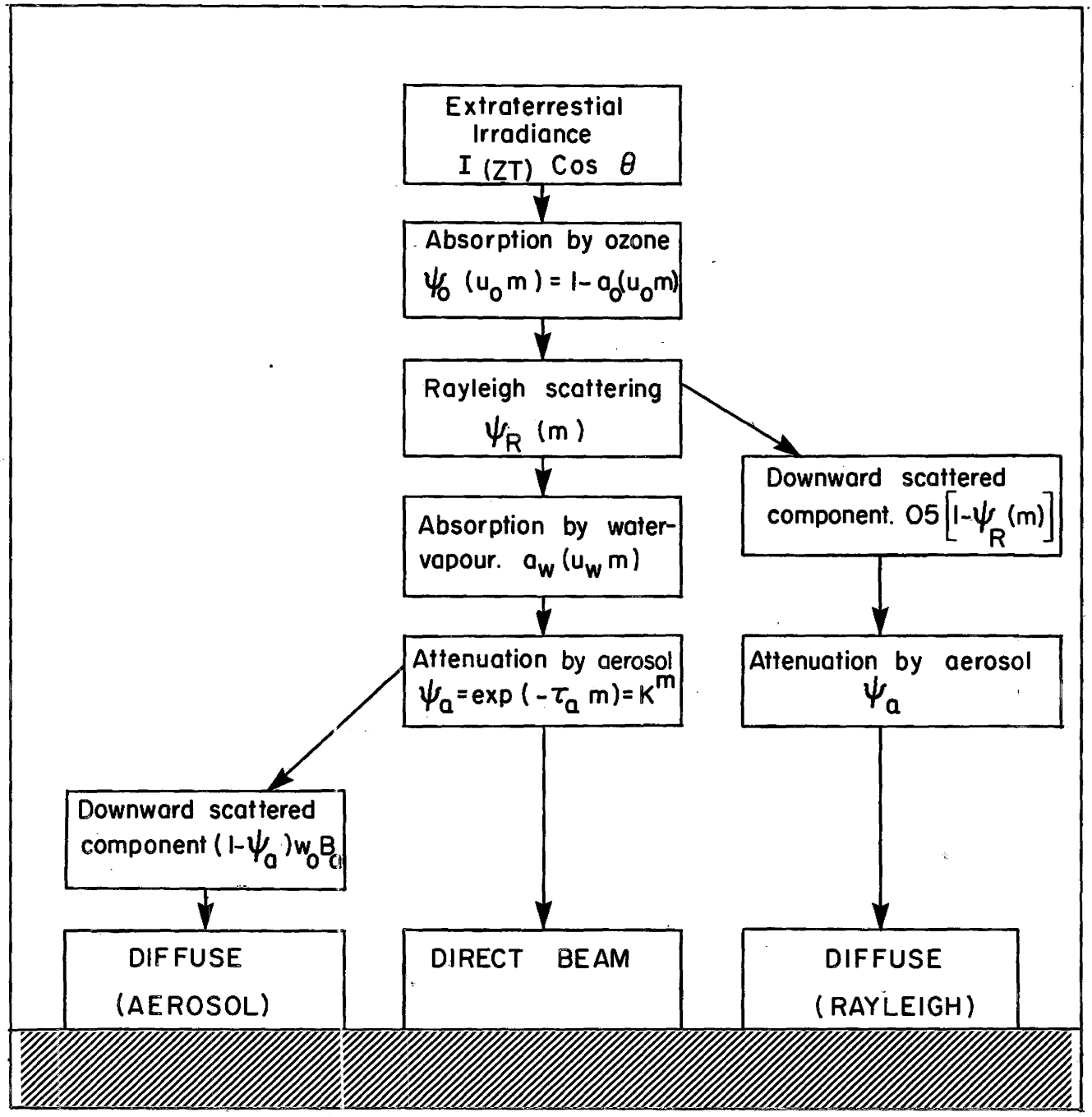

Figure 2 : Model for calculating solar Irradiance and its Direct Beam and Diffuse (aerosol & rayleigh) components.
(After Davies and Hay, 1978)

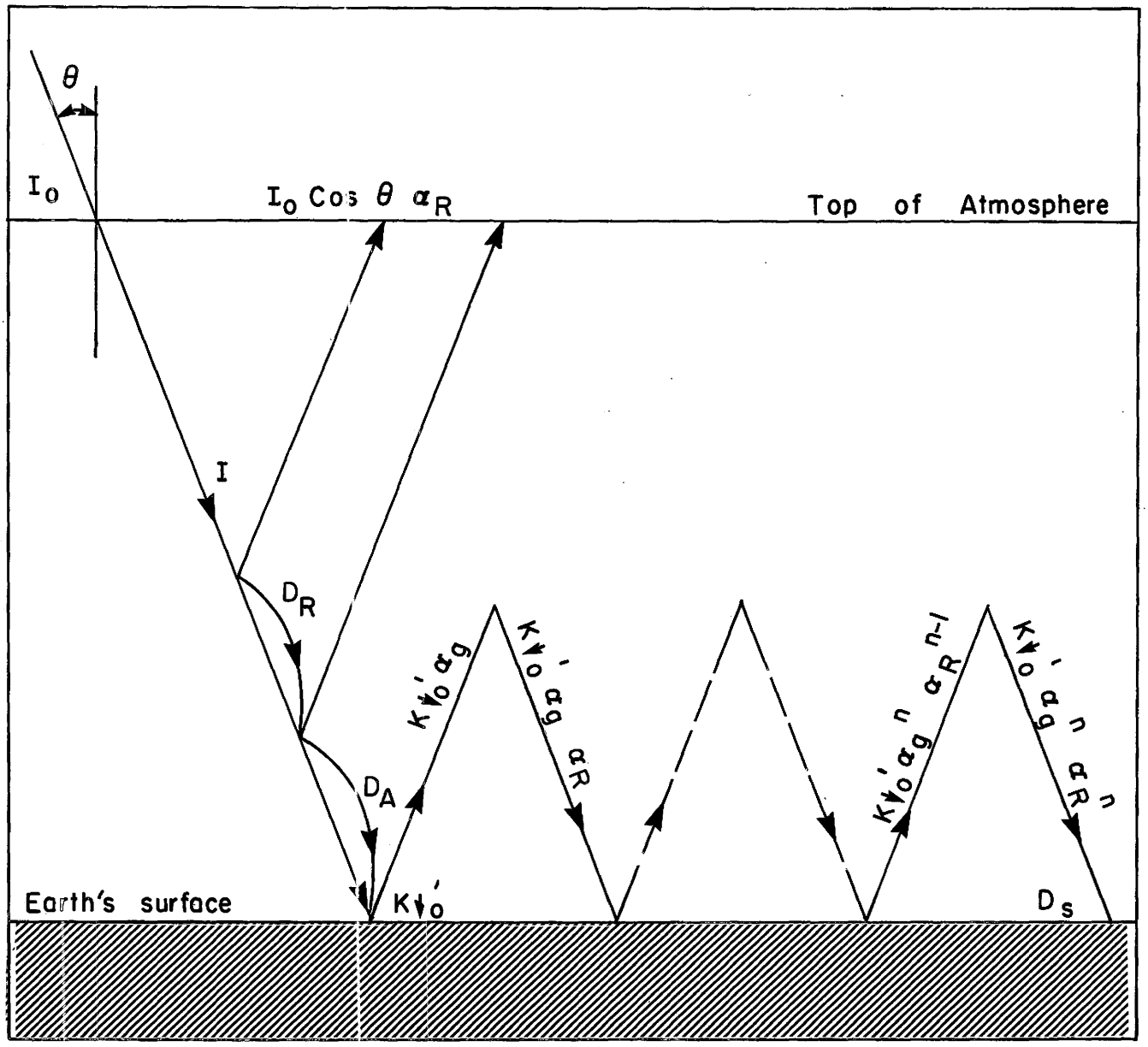

Figure : 2A Cloudless sky schematic diagram for calculating Diffuse Multiply Reflected Radiation.

$K\downarrow_o'$ = global solar radiation before multiple reflection

if $K\downarrow_o$ = actual global solar radiation

$$K\downarrow_o = K\downarrow_o' + K\downarrow_o' \alpha_g \alpha_R + K\downarrow_o' \alpha_g^2 \alpha_R^2 + \ldots\ldots + K\downarrow_o' \alpha_g^n \alpha_R^n = \frac{K\downarrow_o' \alpha_g \alpha_R}{(1 - \alpha_g \alpha_R)}$$

Since $\alpha_g < 1$ and $\alpha_R < 1$, then $\alpha_g^2 \alpha_R^2 \to 0$; $\alpha_g^n \alpha_R^n \to 0$.

$$K\downarrow_o = K\downarrow_o' + K\downarrow_o' \alpha_g \alpha_R$$

$$\psi_{ci} = 1 - (1 - t_i)\, C_i \tag{11}$$

where t_i is the cloud type transmission for the layer and C_i is the amount of cloud. The total transmission of n layers ψ_{cn} is the product of individual layer transmissions:

$$\psi_{cn} = \prod_{i=1}^{n} \psi_{ci} \tag{12}$$

Hence, by combining equations 12 and 11 with equation 10, the surface flux of solar radiation $K\downarrow_c$ can be written as

$$K\downarrow_c = K\downarrow_o \prod_{i=1}^{n} [1-(1-t_i)C_i] \tag{13}$$

The additional component of the surface flux due to surface reflected radiation, which is again reflected back to the surface from a cloud base $K\downarrow_R$ is shown schematically in Figure 3. Assuming that the lowest cloud layer has the predominant effect in this process, it is calculated from

$$K\downarrow_R = K\downarrow_c \; \alpha_c \; \alpha_g \; C_1 \tag{14}$$

where α_c is the reflection coefficient for the cloud base and C_1 is first layer cloud amount as reported by the observer.

Thus, under cloudy sky conditions, solar radiation received at the surface $K\downarrow$ is the sum of equations 13 and 14

$$K\downarrow = K\downarrow_c (1 + \alpha_c \; \alpha_g \; C_1) \tag{15}$$

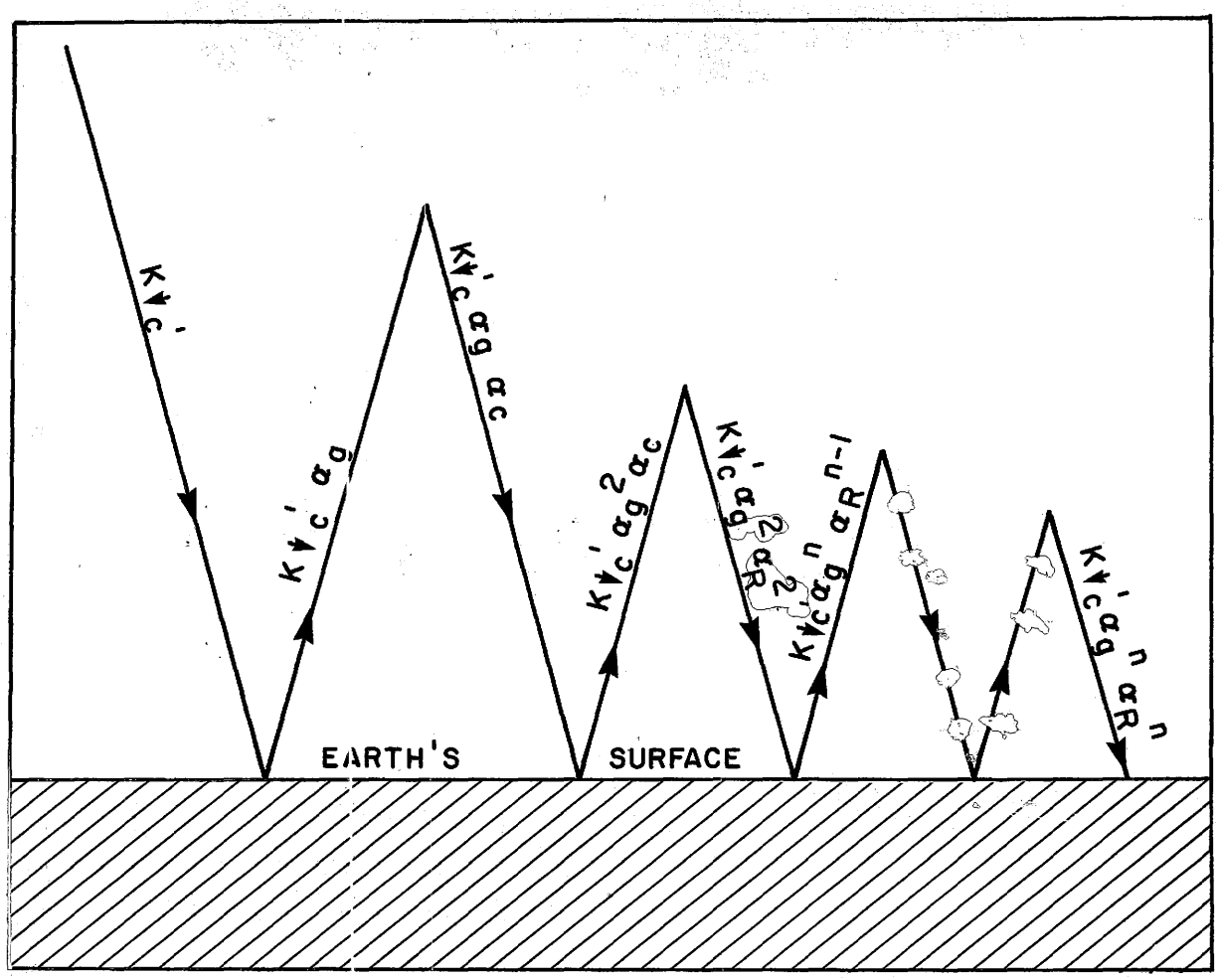

Figure 3 : Schematic diagram for calculating multiple reflection between the Earth's Surface and Cloud Base (after Catchpole and Moodie, 1971)

$K\downarrow_c'$ = cloudy sky global solar radiation before multiple reflection

if $K\downarrow_c'$ = actual cloudy sky global solar radiation

$$K\downarrow_c = K\downarrow_c' + K\downarrow_c' \alpha_g \alpha_c + K\downarrow_c' \alpha_g^2 \alpha_c^2 + \ldots + K\downarrow_o' \alpha_g^n \alpha_c^n = \frac{K\downarrow_c'}{1 - \alpha_g \alpha_c}$$

Since $\alpha_g < 1$ and $\alpha_c < 1$, then $\alpha_g^2 \alpha_c^2 \to 0$; $\alpha_g^n \alpha_c^n \to 0$

$$K\downarrow_c = K\downarrow_c' + K\downarrow_c' \alpha_g \alpha_c$$

CHAPTER 3

SITE, DATA AND CALCULATION PROCEDURES

(A) Experimental Site and Observation Period

Field measurements used in this study were obtained from data published, for 1974, by the Atmospheric Environment Service Department of Environment, Canada (A.E.S.). The instrument site is situated on a flat (slope $> 2^{o}$) gravel plot (15 x 20 m), Figures 4A and 4B. Beyond the instrument plot, most of the land is gently undulating, covered by a mixture of gravel and grass. A.E.S. field laboratories are located to the west (aprox 30 m) of the instrument site (Figure 5).

The selection of the A.E.S. first class station as the study site was based on model and study requirements. These include the following: First, the site be located within an Arctic environment; second, that the radiation sensor records include incoming direct, diffuse and total incoming solar radiation; and thirdly, supplemental meteorological data, such as radiosonde information and hourly cloud observations, should be available within a close proximity to the radiation recording site. All field recording and data reduction was performed by A.E.S. for the full study period, April 1 to August 31, 1974.

(B) INSTRUMENTATION

Global Solar Radiation Flux Density

Incoming solar radiation flux density was measured with an Epply Precision Spectral Pyradometer Model #2 (Epply Laboratory).

Figure 4A Resolute Radiation Sensors, mid-June

Figure 4B Resolute Radiation Sensors, mid-August

(courtesy of Richard Herron)

Figure 5 Photograph of A.E.S. field laboratories at Resolute, (mid-June) (courtesy of Richard Herron)

Diffuse Solar Flux Density

The incoming diffuse solar flux density was measured with an Epply 180 Pyradiometer up until July 1st, 1974.

From July 1, 1974 the flux was measured with a Kipp and Zonen solarimeter.

Direct Solar Flux Density

The incoming direct beam solar flux density was determined as the residual flux between the total and diffuse solar sensor records.

All radiation sensor records were obtained from monthly publications (Monthly Radiation Summary) for hourly periods, converted to S.I. units and stored on computer files.

(C) SUPPLEMENTARY METEOROLOGICAL DATA

In addition to radiation measurements, the A.E.S. Resolute First Class Station also records supplementary meteorological data required for this study. This includes hourly surface cloud observations (both type and amount) and radiosonde data. Radiosonde ascents are made twice daily (00 and 1200 GMT). Daily 00 GMT, the nearest ascent time to solar noon, values were assumed representative of diurnal values in the atmospheric column. Daily values of these parameters were extracted from monthly publications (Canada Upper Air Data, Ozone Data for the World) and transferred to computer cards in S.I. units for subsequent analysis.

Cloud amount and type for the A.E.S. Resolute station were extracted from magnetic tape. Where necessary full twenty-four hour cloud observations, taken for up to four cloud layers, were made at hourly intervals.

(D) PARAMETERIZATION FOR MODEL EVALUATION

Calculations are made at hourly intervals. Values for daily or longer time periods are obtained by summing hourly values.

The irradiance on a unit surface horizontal area at the top of the atmosphere $I_{(ZT)}$ is calculated from

$$I_{(ZT)} = I_0\left(\frac{\bar{d}}{d}\right)^2 \cos\theta$$

where: I_0 = the solar constant at the mean sun-earth distance $\bar{d}$. From Thekaekara and Drummon (1971) it is taken to be 1353 Wm^{-2}.

$\left(\frac{\bar{d}}{d}\right)^2$ = radius vector correction for instantaneous sun-earth distance d.

θ = solar zenith angle defined by

$\theta = \cos^{-1}(\sin\phi\sin\delta + \cos\phi\cos\delta\cosh)$,

in which: ϕ = latitude

ζ = solar declination

h = hour angle as defined by

h = 15/12 - LAT/

where LAT = local apparent time.

Following Lacis and Hansen (1974), ozone absorption $A_{OZ}(x_1)$ is calculated by,

$$A_{OZ}(x_1) = A_{OZ}(x_1)^{vis} + [A_{OZ}(x_1)^{uv}]$$

$$= 0.02118\ x_1 + \left[\frac{1.082}{(1+138.6\ x_1)} + \frac{0.0658\ x_1}{(1+103.6\ x_1)^{\frac{1}{3}}}\right]$$

where: $A_{OZ}(x_1)^{vis}$ = ozone absorption in the visible wavelength band

$A_{OZ}(x_1)^{uv}$ = ozone absorption in the ultra violet wavelength band

x_1 = vertical optical path length for ozone defined by

$x_1 = U_{OZ} \cdot m$,

in which: U_{OZ} = amount to ozone in the vertical columb

m = optical air mass, defined by Kasten (1966) as

$$m = [\cos \theta + 0.15\ (90-\theta) + 3.88]^{-1.253}$$

By definition, transmission of the solar beam due to ozone absorption ψ_{OZ} is

$$\psi_{OZ} = 1 - A_{OZ}\ (x_1)$$

The absorption of water vapour a_{wv}, a function of water vapour amount in the vertical optical path for water X_2, is calculated using Yamamoto's (1962) formula as modified by Lacis and Hansen (1974)

$$a_{wv} = 2.9\ X_2/[(1 + 141.5\ X_2)^{0.633} + 5.925\ X_2],$$

where $X_2 = U_w \cdot m$ and U_w = amount of precipitable water in the vertical columb.

The Rayleigh Optical depth was determined by the metod of Elterman (1968), as recalculated by Davies and Idso (1978) to include an updated depolarization factor of 0.0139 (Hoyt, 1977). Calculated values used for the Rayleigh optical depth τ_R and transmittance ψ_R are linearly interpolated from Table 2 as a function of airmass.

The transmission due to aerosol ψ_a is calculated from

$$\psi_a = k^m,$$

where k = a locally determined constant, to be assigned a value.

The fraction of total radiation scattered by aerosols reaching the ground, B_a, is calculated by interpolating from the experimental data published by Robinson (1962). The values used for this calculation are listed in Table 3 as a function of solar zenith angle.

TABLE 2

Rayleigh optical depth τ_R and transmission ψ_R as a function of airmass m (after Elterman, 1968).

m	τ_R	ψ_R ($\psi_R = e^{-\tau R^m}$)
0.5	0.1305	0.9368
0.7	0.1209	0.9188
1.0	0.1114	0.8946
1.5	0.1006	0.8599
2.0	0.0928	0.8306
2.5	0.0867	0.8051
3.0	0.0871	0.7826
4.0	0.0738	0.7443
6.0	0.0630	0.6852
8.0	0.0557	0.6406
10.0	0.0502	0.6051
12.0	0.0460	0.5757
16.0	0.0398	0.5294
20.0	0.0353	0.4938
25.0	0.0312	0.4589
30.0	0.0281	0.4309

TABLE 3

Ration values of forward to total scattering (B_a) by aerosol, as a function of solar zenith angle (after Robinson, 1962).

Solar zenith angle	B_a values
0.0	0.92
25.8	0.91
36.9	0.89
45.6	0.86
51.3	0.83
60.0	0.78
66.4	0.71
72.5	0.67
78.5	0.60

The multiply reflected contribution to the diffuse flux requires that values for surface and atmospheric albedo's be specified. Regional surface albedo's along with those used in this study are given in Table 4 as a function of location. Atmospheric albedo is calculated according to the approach adopted by Davies and Hay (1978). It is defined by

$$\alpha_R = \alpha_a^* + \alpha_R^*/2$$

where α_a^* = reflection co-efficient due to aerosol backscattering, and can be taken as

$\alpha_a^* = 1 - B_a = 0.15$

α_R^* = reflection co-efficient due to Rayleigh backscattering of surface reflected radiation, and obtained from Lacis and Hansen (1974) as $\alpha_R^* = 0.0685$

Under cloudy sky conditions, the model is evaluated for up to 4 layers of cloud and requires estimates for the fractional cloud amount in each layer. Cloud observations (cloud amount and type) taken by Atmospheric Environment Services (A.E.S.) at Resolute report cloud amount for up to 4 layers as a fraction of the total cloud amount. These observations are corrected for use in the model according to the procedure of Davies et al. (1975).

$$Ci = Ci^1/(1 - \sum_{i=n}^{i+1} Ci^1)$$

where Ci = corrected cloud amount in layer i

Ci^1 = cloud amount in layer i as reported by A.E.S.

$\sum_{i=n}^{i+1} Ci^1$ = the sum of reported cloud amount in the layers beneath the top layer

Figure 6 illustrates the cloud layer correction procedure employed.

Cloud transmittance is calculated according to

TABLE 4

Monthly mean values of surface albedo α_g (summarized by Hay, 1976) and those assigned to 1974 Resolute data.

	Monthly mean α_g					
	Toronto Met. Resources	Toronto Scarborough	Montreal, Jean Brebeuf	Goose Bay	Resolute	Assigned to Resolute 1974 Data
January	0.50	0.50	0.32	0.55	0.80	
February	0.50	0.50	0.33	0.56	0.80	
March	0.38	0.38	0.25	0.50	0.79	
April	0.28	0.28	0.22	0.50	0.76	0.80
May	0.25	0.25	0.20	0.35	0.69	0.70
June	0.25	0.25	0.20	0.25	0.45	0.60
July	0.25	0.25	0.20	0.25	0.26	0.30
August	0.25	0.25	0.20	0.25	0.21	0.30
September	0.25	0.25	0.20	0.25	0.45	
October	0.25	0.25	0.20	0.30	0.59	
November	0.29	0.28	0.23	0.35	0.74	
December	0.39	0.39	0.28	0.52	0.79	

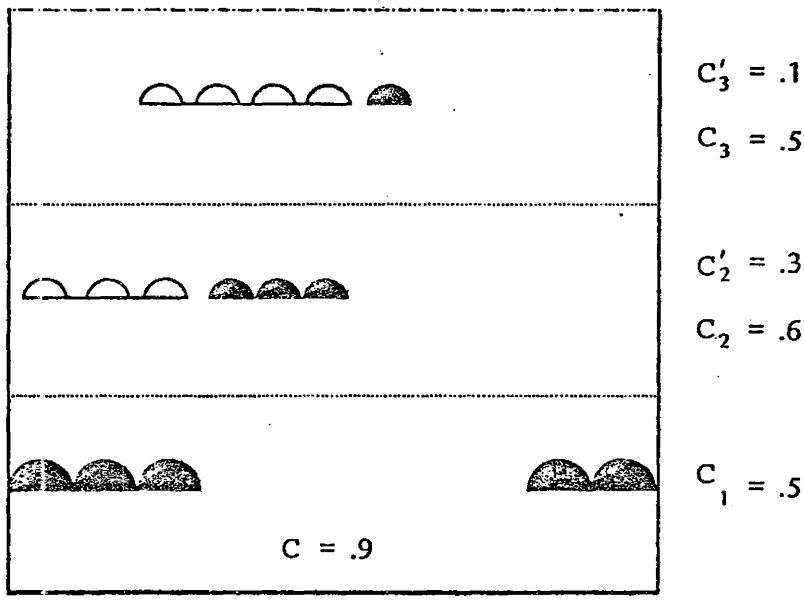

Figure : 6 Example of the correction for cloud layer amounts in layer partially obstructed by lower cloud. (after Suckling and Hay, 1977)

$$t_i = \frac{a}{K\downarrow_o m} \exp(-bm)$$

where a, b = constants specified by cloud type as defined in Table 5 based on Haurwitz (1948).

TABLE 5

Haurwitz cloud type transmission constants and constants assigned to Resolute cloud data

Cloud Type	Haurwitz a ($kWhm^{-2}hr^{-1}$)	Haurwitz b	Assigned a (Wm^{-2})	Assigned b
F	0.1786	0.028	0.179	0.028
St	0.2761	0.159	0.276	0.159
Sc	0.4025	0.104	0.403	0.104
Cu			0.403	0.104
Cb			0.403	0.104
As	0.4524	0.063	0.452	0.063
Ac	0.6090	0.112	0.609	0.117
Ci	0.9535	0.079	0.954	0.079
Cs	1.0104	0.148	1.010	0.148
Sf			0.276	0.159
Cf			0.403	0.104
Cut			0.403	0.104
Ns	0.1299	-0.167	0.130	-0.167
Acc			0.609	0.112
CC			1.010	0.148
Obs other than fog			0.179	0.028

CHAPTER 4

RESULTS AND DISCUSSION

(A) INTRODUCTION

In this chapter, the results from cloudy and cloudless sky model performance are presented. Cloudless model performance will be examined and discussed first. The effect of aerosols on calculated surface flux values is also considered.

(B) EVALUATION OF DUST TRANSMISSION

The depletion of direct beam radiation in a cloudless atmosphere, after absorption by ozone, is primarily the result of absorption by water vapour and absorption and scattering by aerosols. Davies et al. (1975) showed that large variations in atmospheric water vapour content lead to minor variations in calculated flux values (Figure 7).

The atmospheric aerosol content above a surface depends, firstly; on local weather conditions, which determine aerosol inputs from local sources, and secondly; on the prevailing air mass which determines inputs from distant sources. For Resolute, the latter is dominated by relatively clean Arctic sea air masses. Local sources include smoke, haze and dust generated by nearby airport traffic.

In the absence of atmospheric aerosol data, aerosol effects on direct beam transmissions were evaluated by varying the aerosol loading coefficient (k) to minimize differences between measured and computed cloudless sky values.

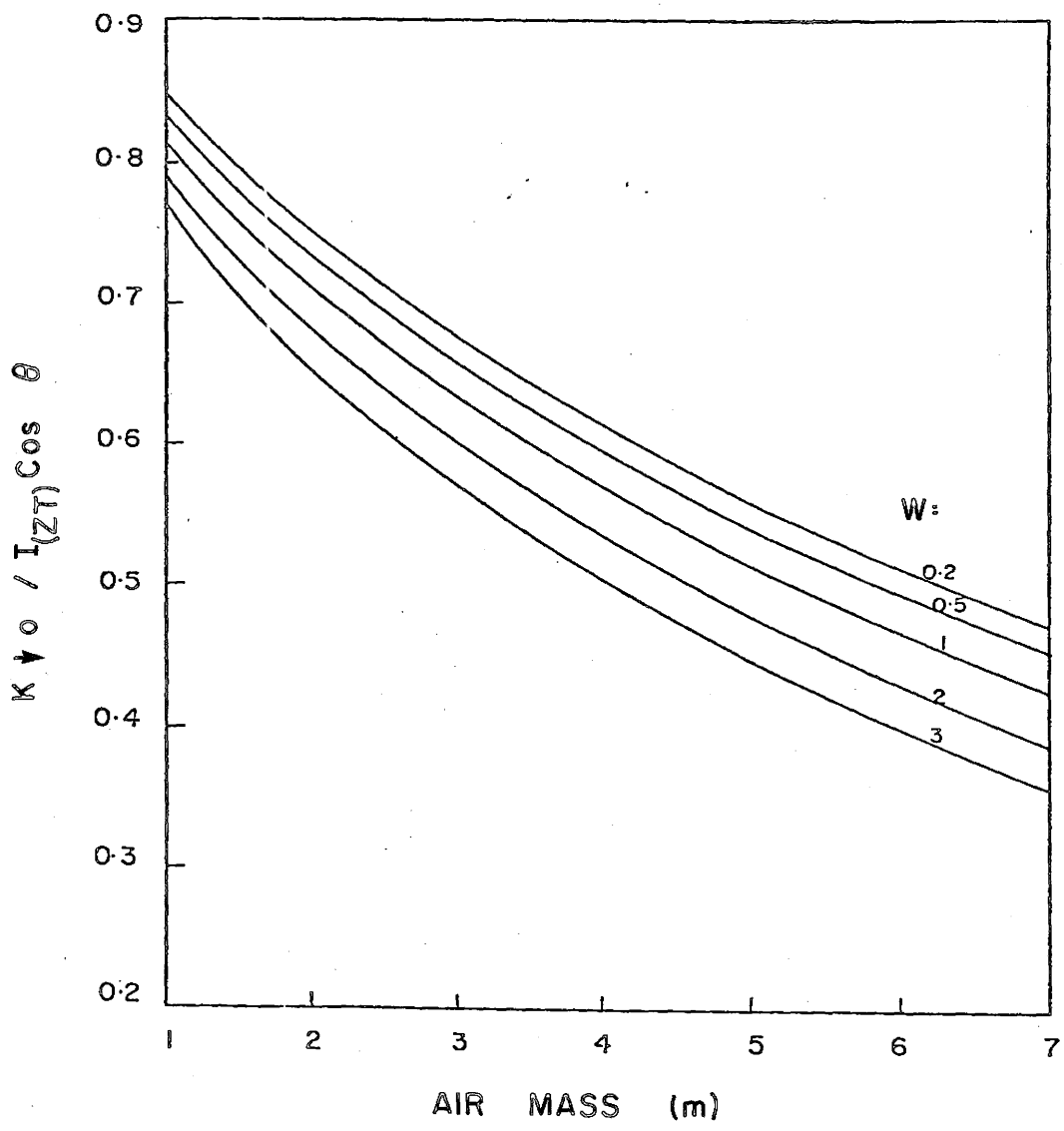

Figure : 7 Dependence of cloudless sky estimates of global solar radiation upon precipitable water.
(After Davies et al., 1975)

During the study period, the lack of cloudless days with complete radiation sensor records forced the adoption of nearly cloudless days and part days for cloudless sky analysis. Only three nearly cloudless days and six other days of nearly cloudless periods were found from cloud records at the adjacent meteorological station. For these days, radiation totals were computed for four tried values (k=0.98, 0.91, 0.88, 0.86). The results, along with measured values and cloud conditions are presented in Table 6. Differences between measured and observed values (Table 6, Figure 8) show that no particular aerosol loading coefficient value predominated. On the three nearly cloudless days, differences between measured and calculated solar radiation values were minimized using k=0.91 (2 of 3 cases). For the remaining six nearly cloudless periods, best agreement was equally partitioned between k=0.91 and lower (k) values. Calculated values using k=0.91 (Figure 8) generally overestimate (8 of 9 cases) observed direct beam values. Largest absolute differences between computed and observed values occurred with k=0.98.

Eighteen nearly cloudless hours, where mean cloud amount was less than 1/10, were also considered (Table 7). For these hours, best agreement between measured and observed values were obtained using k=0.88 (10 of 18 cases). For the remaining eight single hour periods, better agreement (observed-calculated) was equally partitioned between k=0.91 and k=0.86 (Figure 9). This suggests that k=0.88 is an acceptable value for use in cloudless sky conditions, at Resolute.

TABLE 6

Measured and computed nearly cloudless direct beam solar radiation values at various k and data criteria. Complete solar day indicated by +. Best (measured-computed) agreement indicated by *.

Date	Time (LAT)	Mean hourly cloud amount	Hourly cloud amount (per layer)	Cloud type (per layer)	Measured (Wm^{-2})	Direct Solar (Wm^{-2}) Calculated and Measured-calculated % difference			
						k=0.98	k=0.91	k=0.88	k=0.86
4/1/74 +	6		.1	Ci					
	7		.1	Ac	5.319	8.847	6.607	5.818	5.338
	8		.1/.1	Sc/Ci		-39.9%	-19.5%	-8.6%	-0.4%
	9		.1/.1	Sc/Ci		(% difference from measured)			
	10		.1/.1	Sc/Ci					
	11		.1	Ci					
	12	.1	.1	Ci					
	13	.1	.1	Cs					
	14		.1/.1	Cf/Cs					
	15		.1	Cf					
	16		.1	Cu					
	17		.1	Cu					
	18		.1	Sc					
	19		.1	Sc					
4/10/74	5				6.910	8.801	*6.949	6.265	5.840
	6					-21.5%	-0.6%	10.3%	18.3%
	7								
	8								
	9								
	10								
	11								
	12								
	13		.1	Ci					

6/25/74	7		.1/.1	Sc/Ac	23.913	28.689	*24.464	22.797	21.731
	8		.1/.1	Sc/Ac		-16.6%	-2.3%	4.9%	10.0%
	9		.1/.1	Sc/Ac					
	10		.1	Sc					
	11		.1	Sc					
	12		.1/.1	Sc/Ac					
	13		.1/.1	Sc/Ac					
	14		.1/.1	Sc/Ac					
	15		.1/.1	Sc/Ac					
	16		.1	Ac					
	17		.1/.1	Cf/Ac					
	18		.1/.1	Sc/Ac					
	19		.1	Sc					
	20		.1/.1	Cf/Sc					
	21		.1	Sc					
	22		.1	Sc					
	23		.1/.1	Sc/Ac					
	24		.1/.1	Sc/Ac					
6/26/74 +	1		.1/.1	Sc/Ac	26.929	32.920	*27.603	25.547	24.243
	2		.1/.1	Sc/Ac		-18.2%	-2.4%	5.4%	11.1%
	3		.1/.1	Sc/Ac					
	4		.1	Sc					
	5		.1/.1	Sf/Sc					
	6		.1/.1	Sf/Sc					
	7		.1/.1	St/Sc					
	8		.1/.1	Cf/Sc					
	9		.1	Sc					
	10	.1	.1	Sc					
	11	.1	.1	Sc					
	12	.1	.1	Sc					
	13		.1	Sc					
	14		.1	Sc					
	15		.1/.1	Sc/Ac					
	16		.1/.1	Sc/Ac					
	17	.1	.1/.1	Sc/Ac					
	18	.1	.1/.1	Sc/Ac					
	19		.1/.1	Cf/Sc					
	20		.1/.1	Cf/Ac					
	21		.1/.1	Cf/Ac					
	22		.1/.1	Sc/Ac					
	23		.1/.1	Sc/Ac					
	24		.1/.1	Sc/Ac					

Table 6 continued ....

6/27/74	1	.1/.1	Sc/Ac	13.443	16.789	14.099	*13.057	12.396
	2	.1/.1	Sc/Ac		-19.9%	-4.7%	3.0%	8.4%
	3	.1	Ac					
	4	.1	Ac					
	5	.1/.1	Sc/Ac					
	6	.1/.1	Sc/Ac					
	7	.1/.1	Sc/Ac					
	8	.1	Ac					
	9	.1	Ac					
	10	.1	Ac					
	11	.1	Ac					
	12	.1	Ac					

Table 6 continued ....

7/12/74	9		.1	Ac	8.837	11.060	9.726	9.177	*8.818
	10		.1	Ac		-20.1%	-9.1%	-3.7%	0.2%
	11		.1	Ac					
	12		.1	Ac					
	13		.1	Ac					
7/29/74	3		.1/.1	Ac/Ci	8.166	10.518	8.639	*7.923	7.472
	4		.1/.1	Ac/Ci		-22.4%	-5.5%	3.1%	9.3%
	5		.1/.1	Ac/Ci					
	6		.1/.1	Ac/Ci					
	7		.1	Ac					
	8		.1	Ac					
	9		.1/.1	Ac/Ci					
	10		.1/.1	Ac/Ci					
	11		.1/.1	Ac/Ci					
8/22/74	10		.1	Sc	6.491	7.757	*6.560	6.081	5.773
	11		.1	Sc		-16.3%	-1.1%	6.7%	12.4%
	12		.1	Sc					
	13		.1	Sc					
	14		.1	Sc					
8/25/74 +	4		.1	Ci	12.731	15.240	*12.108	10.953	10.237
	5		.1	Ci		-16.5%	5.1%	16.2%	24.4%
	6		.1	Ci					
	7								
	8								
	9								
	10								
	11								
	12		.1	Sf					
	13		.1	Sf					
	14		.1	Cu					
	15								
	16		.1	Ci					
	17		.1	Ci					
	18		.1	Ci					
	19	.1	.1	Ci					
	20		.1	Ci					
	21	.1	.1	Ci	112.739	140.621	116.755	107.618	101.848
						-19.8%	-3.4%	4.7%	10.7%

Table 6 continued ....

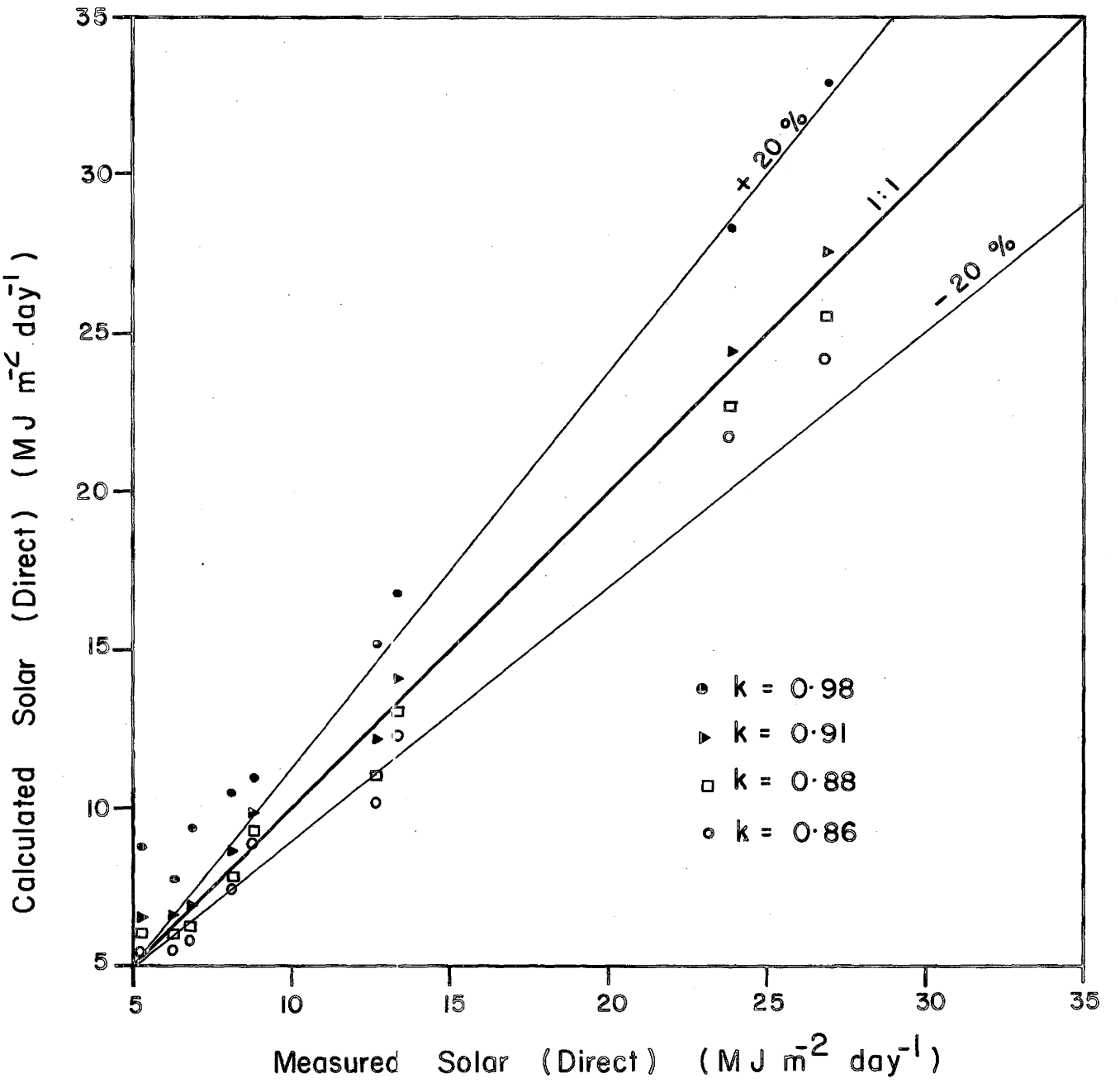

Figure 8 : Correlation between observed and calculated nearly cloudless Direct Beam solar radiation for daily periods at various aerosol coefficient (k) values.

TABLE 7

Hourly measured and calculated cloudless, and nearly cloudless, incoming direct beam solar radiation at various aerosol coefficient values. Best agreement indicated by *.

Date	Time (LAT)	Total hourly cloud cover	Layer cloud amount	Cloud type	Direct Solar (Wm^{-2}) Measured (Wm^{-2})	Calculated and Measured-calculated % difference k=0.98	k=0.91	k=0.88	k=0.86
4/1/74	11		.1	Ci	197.8	286.0 -30.8%	227.0 -12.9%	*204.5 -3.3%	190.4 3.9%
4/3/74	14				221.0	294.8 -25.0%	235.1 -6.0%	*212.3 4.1%	197.9 11.7%
4/4/74	12		.1	Ci	232.7	326.9 -28.8%	265.8 -12.5%	241.5 -3.6%	*226.4 2.8%
4/9/74	11		.1	Ci	279.2	349.1 -20.0%	284.7 *-1.9%	261.1 6.9%	245.4 13.8%
4/10/74	12				290.8	374.4 -22.3%	308.9 -5.9%	*284.6 2.2%	268.3 8.4%
4/11/74	12		.1/.1	Sc/Ci	221.0	382.7 -42.3%	316.0 -30.1%	292.1 -24.3%	*275.7 -19.8%
4/22/74	11		.1	Sc	325.7	443.2 -26.5%	375.4 -13.2%	347.8 -6.4%	*330.3 -1.4%
4/28/74	10		.1	Sc	360.6	446.6 -19.3%	378.5 -4.7%	*350.9 2.8%	333.3 8.2%

4/30/74	12		.1/.1	Sc/Ac	418.8	510.9 -18.0%	443.2 -5.5%	*412.0 1.7%	393.5 6.4%
6/25/74	11		.1	Sc	558.4	662.1 -15.7%	586.4 -4.8%	*555.1 0.6%	534.7 4.4%
6/26/74	12	.1	.1	Sc	570.0	679.0 -16.1%	603.0 -5.5%	*571.5 -0.3%	550.9 3.5%
6/27/74	12		.1	Ac	570.0	681.6 -16.4%	605.4 -5.8%	*573.5 -0.6%	553.0 3.1%
7/12/74	12		.1	Ac	523.5	653.5 -19.9%	578.4 -9.5%	547.3 -4.3%	*526.9 -0.6%
7/29/74	12	.1	.1	Ac	488.6	588.7 -17.0%	515.7 -5.3%	*486.1 0.5%	466.6 4.7%
8/1/74	11		.1	Sf	465.3	552.5 -15.8%	482.1 -3.5%	*451.7 3.0%	432.7 7.5%
8/22/74	12		.1	Sc	383.9	451.9 -15.0%	*384.9 -0.3%	357.4 7.4%	340.0 12.9%
8/24/74	12		.1/1.	Sf/Ci	372.3	436.4 -14.7%	*370.1 0.6%	343.3 8.4%	326.1 14.2%
8/25/74	12		.1	Sf	372.3	436.1 -14.6%	*368.9 0.9%	342.1 8.8%	324.8 14.6%
					Σ =6851.9	8556.4 -19.9%	7329.5 -6.5%	6834.8 0.2%	6516.9 5.1%

Table 7 continued ....

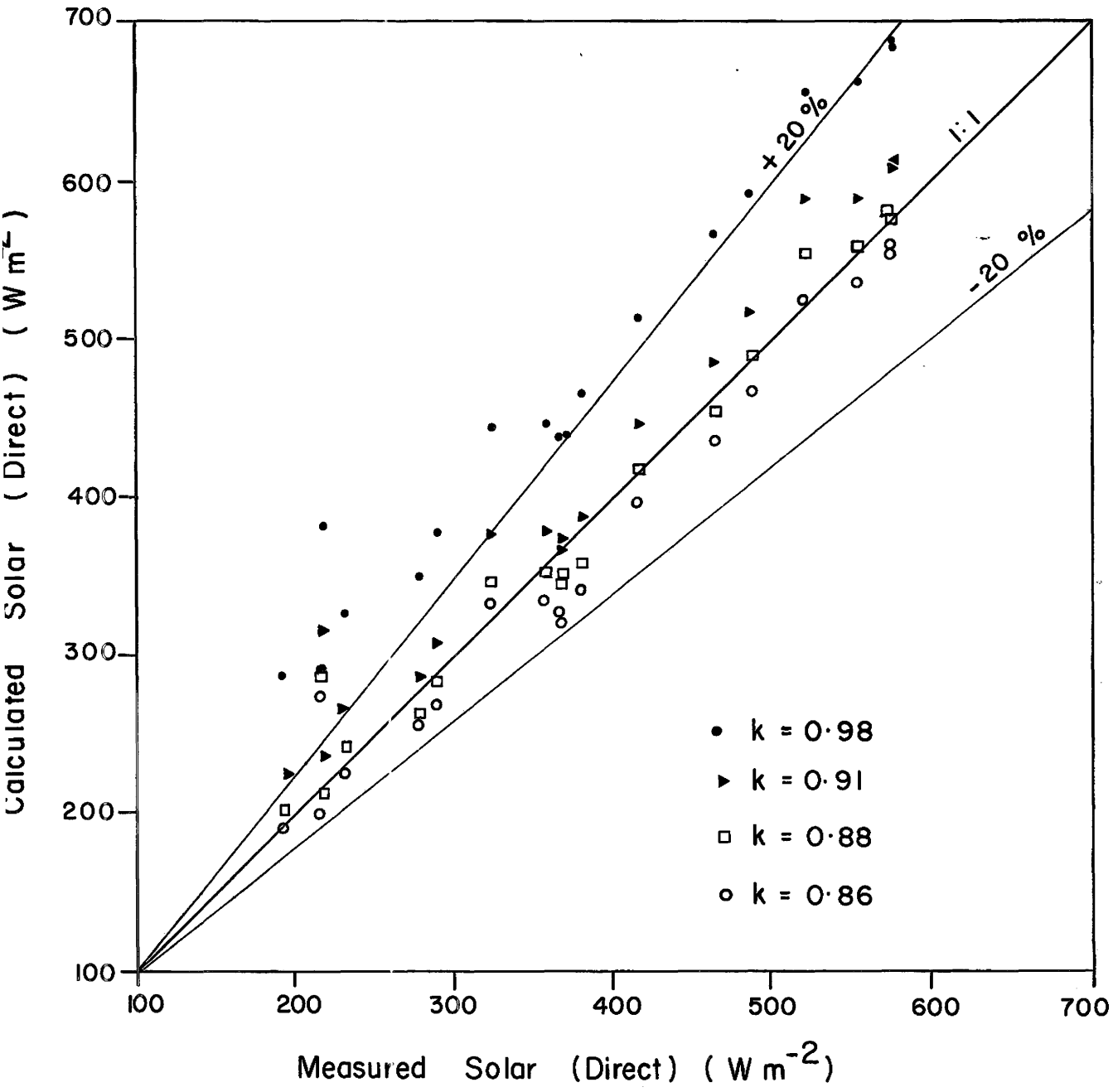

Figure 9 : Correlation of hourly observed and calculated Direct Beam solar radiation for different aerosol coeffecient (k) values. Results refer to nearly cloudless periods.

(C) EVALUATION OF CLOUDLESS SKY SOLAR RADIATION (k=0.88)

The relative quantity of diffuse radiation incident at the surface under cloudless sky conditions is generally less than 20% (Davies and Hay, 1978) of the total solar flux. Hence, the error in calculated solar radiation should be similar to that of direct beam values. This hypothesis was tested by comparing measured and calculated solar radiation values for the 18 nearly cloudless hours, since they represent the greatest seasonal variation.

Despite the use of hourly rather than daily values, Figure 10 and Table 8 show that the cloudless sky model yields errors of small relative magnitude. In relative terms, errors of less than 10% for 94% of the hourly values were found. Table 8 also indicates that there is a systematic tendency for the model to overestimate the diffuse flux density. One possible explanation for this systematic error is that the value used for the single scattering albedo (W_o = 0.98) was too high. The use of W_o = 0.98 suggests the presence of an almost purely scattering atmosphere (Toon and Pollack, 1976). This would also suggest that k = 1.0. However, since k=0.88 gave best measured-calculated agreement, the use of a lower W_o value would seem appropriate. Bergstrom and Petterson (1977) suggest the use of values between W_o = 0.6 and 0.8 for areas of similar aerosol conditions indicated by k=0.88.

(D) EVALUATION OF CLOUDY SKY DUST TRANSMISSION

Under a variety of cloud conditions, Davies et al. (1975) found that for several southern Ontario sites a larger aerosol coefficient applied

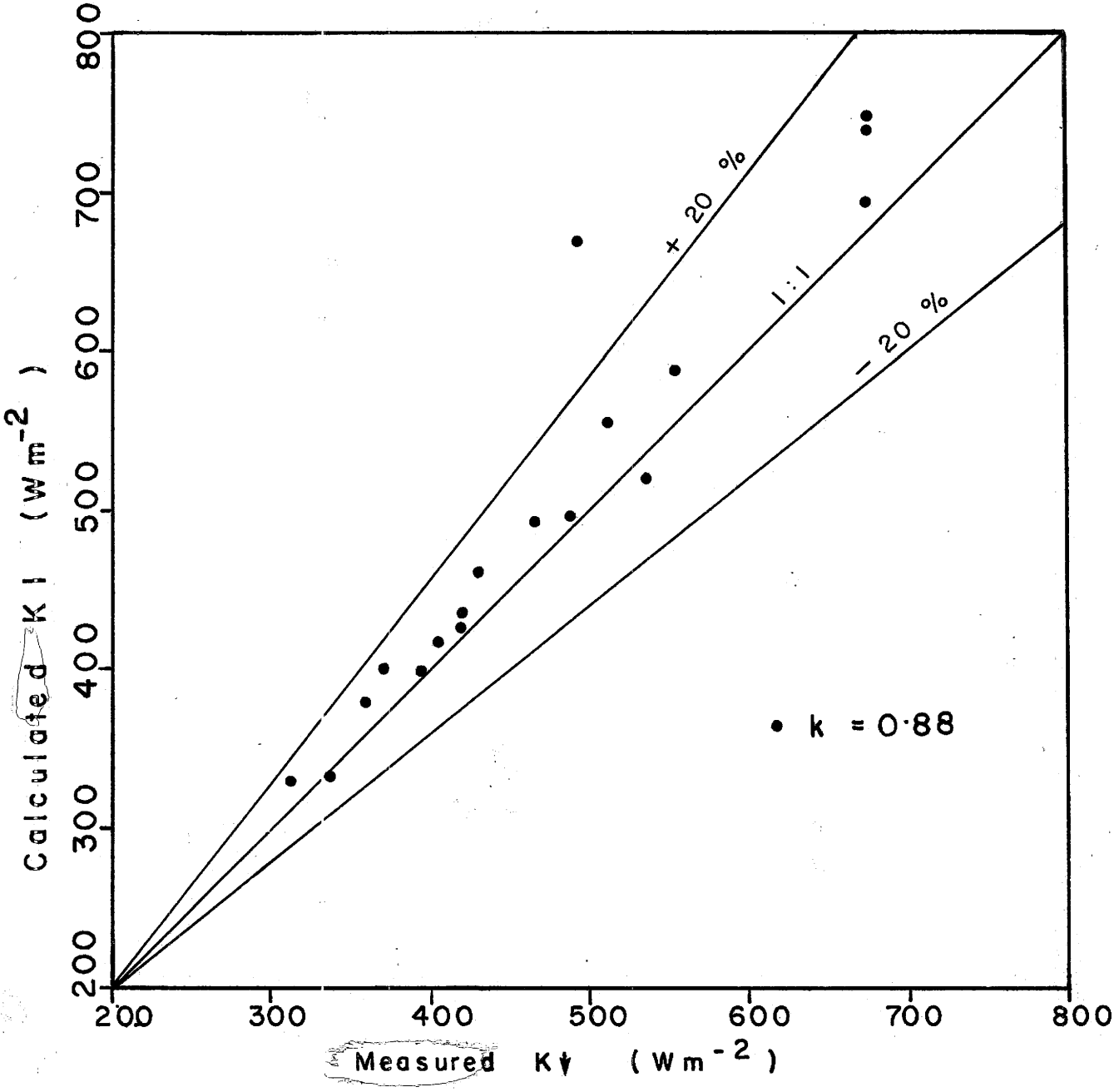

Figure 10: Correlation of hourly observed and calculated solar radiation (K↓) for cloudless and nearly cloudless sky conditions

TABLE 8

Comparison of hourly measured and calculated solar radiation for cloudless and nearly cloudless sky conditions.

Date	Time	Measured $K\downarrow$ (Wm^{-2})	Calculated $K\downarrow$ (Wm^{-2})	Measured-calculated % difference	Direct beam measured-calculated % difference	% Diffuse flux of $K\downarrow$
4/1/74	11	314.1	329.7	-4.7	-3.3	37.0
4/3/74	14	337.4	335.2	1.0	4.1	34.5
4/4/74	12	360.6	380.8	-5.3	-3.6	35.5
4/9/74	11	395.5	299.6	-1.0	6.9	29.4
4/10/74	12	407.2	418.9	-2.8	2.2	28.6
4/11/74	12	372.3	401.0	-7.1	-24.3	40.6
4/22/74	11	465.3	492.2	-5.5	-6.4	30.0
4/28/74	10	488.6	496.1	-1.5	2.8	14.3
4/30/74	12	535.1	518.2	3.3	1.7	21.7
6/25/74	11	674.7	694.6	-2.8	0.6	17.2
6/26/74	12	674.7	739.0	-8.7	-0.3	15.5
6/27/74	12	674.7	748.8	-9.9	-0.6	15.5
7/12/74	12	593.3	668.7	-11.2	-4.3	11.7
7/29/74	12	546.8	588.6	-7.1	0.5	10.6
8/1/74	11	511.9	556.7	-8.0	3.0	9.1
8/22/74	12	430.4	459.0	-6.2	7.4	10.8
8/24/74	12	418.8	427.7	-2.1	8.4	11.1
8/25/74	12	418.8	432.2	-3.1	8.8	11.1

than that used for cloudless skies. To determine if this effect was also a characteristic of Resolute, the aerosol coefficient was varied to determine the locally suited value under cloudy sky conditions. From several trials, k=0.91 and k=0.88 were selected since they produced best agreement between measured and observed radiation values. Of the twenty-nine days (indicated in Table 9) selected for this analysis, best agreement, presented in Figure 11, was obtained with k=0.88 on 17 of the 29 days. Table 9 and Figure 11 indicate that discriminating between using k=0.88 or k=0.91 is difficult since daily calculated values show less than 5% variation. However, the use of a similar aerosol coefficient for cloudless and cloudy sky conditions is indicated for Resolute.

In computations involving clouds, deviations from measured values using k=0.91 or k=0.88 become less important when compared to the greater attenuation effect of cloud presence. Differences between the actual surface solar flux and that possible under cloudless conditions is dominantly a function of characteristic cloud type radiative properties.

(E) ANALYSIS OF MODEL PERFORMANCE WITH TIME

Atmospheric cloud conditions and a comparison of the computed and observed daily solar fluxes are presented in Figure 12 for the full study period (April 1 to August 31, 1974). In general, Figure 12 indicates a tendency of model underestimation of observed values from the beginning of May through to about the twentieth of June. Better model performance occurs otherwise. With k=0.88, Table 10 indicates that on a daily basis, measured and calculated values agree to within $\pm$ 20% on about 55% of the days. For the five day and monthly mean values, Figure 13 (Table 11)

TABLE 9

Daily measured and calculated cloudy sky solar radiation at various aerosol coefficient values. Best agreement indicated by *.

Date	Measured $K\downarrow$ (Wm^{-2})	Calculated $K\downarrow$ (Wm^{-2}) k=0.91	Measured-calculated % difference k=0.91	Calculated $K\downarrow$ (Wm^{-2}) k=0.88	Measured-calculated % difference k=0.88	Mean daylight cloud amount
4/2/74	10.117	10.642	-4.9	10.266*	-1.5	.29
4/8/74	12.187	12.240*	-0.4	11.830	3.0	.23
4/9/74	12.396	14.016	-11.6	13.618*	-9.0	.38
5/14/74	22.070	18.833*	17.2	18.439	19.7	.47
5/16/74	25.463	26.899	-5.3	26.288*	-3.1	.25
6/8/74	29.107	32.380	-10.1	31.892*	-8.7	.41
6/17/74	34.886	31.153*	12.9	30.560	14.2	.27
6/20/74	32.750	36.883	-11.2	36.445*	-10.1	.52
6/21/74	31.829	35.957	-11.5	35.567*	-10.5	.89
6/22/74	27.431	19.938*	37.58	19.801	38.5	.93
6/23/74	30.363	31.209	-2.7	30.974*	-1.9	.79
6/24/74	29.651	27.069*	9.5	26.718	11.0	.55
6/28/74	33.127	30.464*	8.7	30.065	10.2	.38
6/29/74	31.871	34.388	-7.3	33.835*	-5.8	.32
7/10/74	27.892	27.641*	0.9	27.343	2.0	.43
7/11/74	27.934	31.469	-11.2	31.191*	-10.4	.43
7/27/74	22.113	24.596	-10.1	24.214*	-8.7	.59
7/29/74	20.731	25.219	-17.8	24.978*	-17.0	.45
7/31/74	14.700	10.851*	35.5	10.758	36.6	.87
8/2/74	14.700	14.918	-1.5	14.856*	-0.9	.92
8/3/74	9.088	12.751	-28.7	12.619*	-27.9	.79
8/4/74	17.422	18.189	-4.2	17.953*	-3.0	.47
8/22/74	15.454	16.436	-6.0	16.186*	-4.5	.30
8/26/74	12.732	12.251*	3.9	12.119	5.1	.62
8/27/74	9.339	9.628	-3.0	9.469*	-1.4	.59
8/28/74	11.140	10.189*	9.3	10.007	11.3	.55
8/29/74	12.690	10.909*	16.3	10.729	18.3	.44
8/30/74	12.650	11.144*	13.5	10.933	15.7	.37
8/31/74	10.051	11.638	-13.6	11.515*	-12.7	.66

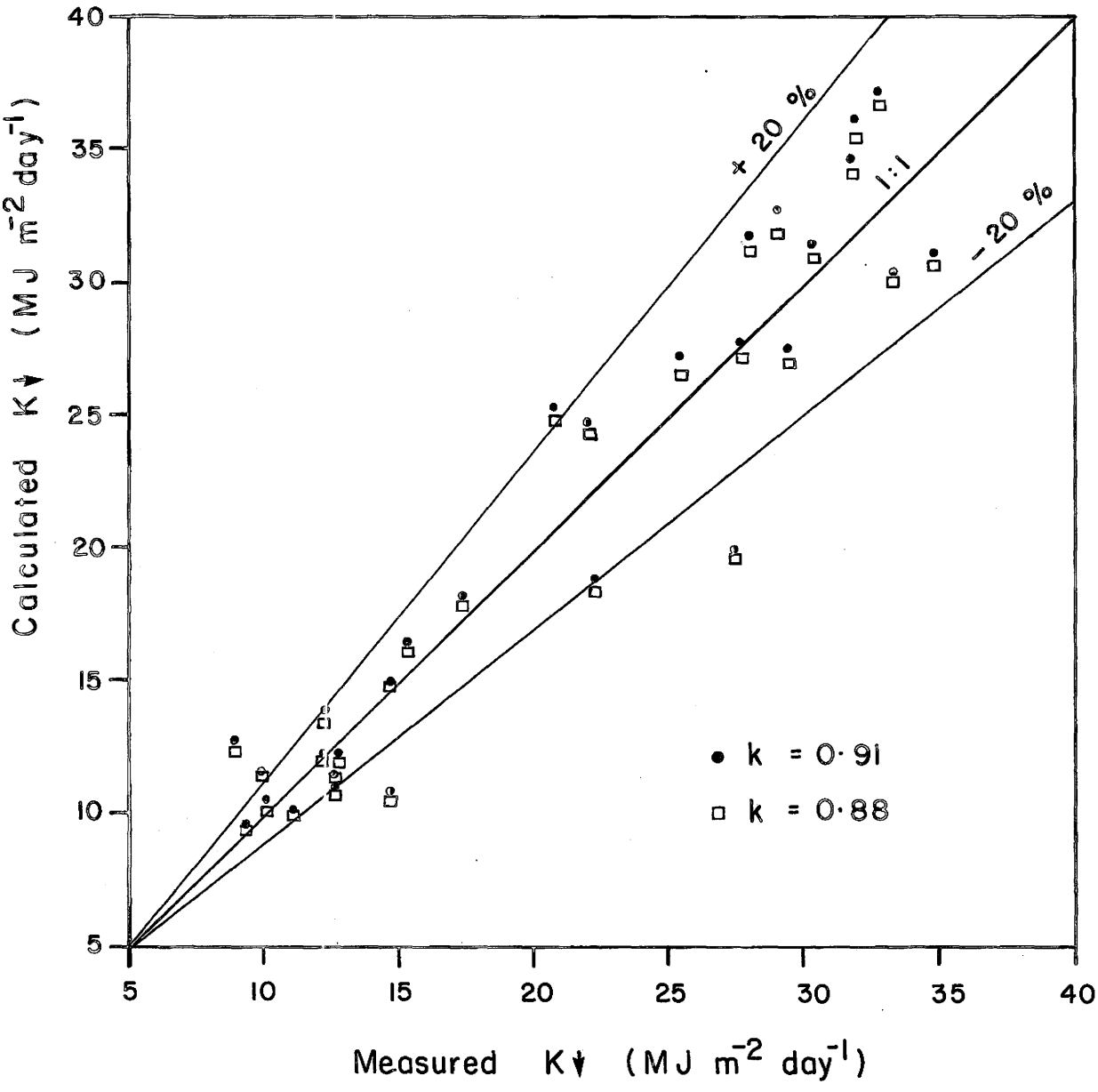

Figure 11 : Correlation between measured and calculated daily values of cloudy sky solar radiation (K↓) for different aerosol coeffecient (k) values

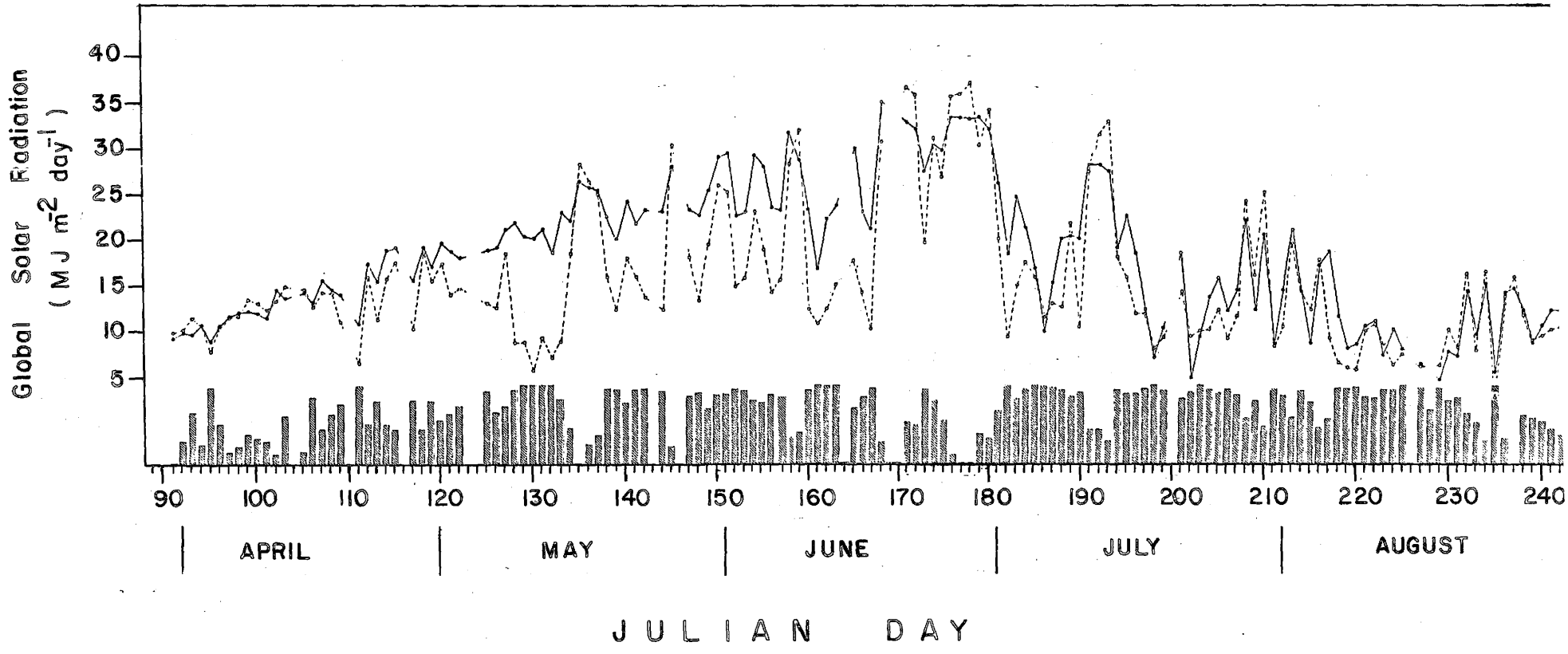

Figure 12 : Comparison of daily measured and calculated Global solar radiation with mean daily cloud amount.

TABLE 10

Percentage difference between daily totals of measured and calculated solar radiation at Resolute for full study period

Date	Measured-calculated % difference	Date	Measured-calculated % difference
April		May	
1	-4.1	1	32.3
	nearly cloudless	2	21.9
2	-1.5	3	
3	-15.9	4	
4	-0.2	5	42.0
5	12.1	6	50.2
6	1.9	7	15.0
7	1.5	8	85.7
8	3.0	9	68.5
9	-9.0	10	145.2
10	-8.4	11	69.7
	nearly cloudless	12	147.8
11	-6.2	13	
12	9.2	14	
13	-1.5	15	-6.5
14		16	-3.1
15	-1.5	17	2.6
16	4.1	18	38.8
17	8.7	19	58.7
18	2.0	20	32.9
19	24.8	21	34.9
20		22	66.2
21	61.7	23	
22	8.3	24	81.3
23	35.4	25	-7.2
24	19.6	26	
25	9.7	27	25.4
26		28	66.3
27	46.7	29	29.4
28	3.7	30	11.7
29	10.4	31	17.0
30	12.7		

Table 10 continued ....

June		July	
1	51.3	1	86.5
2	43.5	2	62.6
3	26.0	3	22.1
4	45.5	4	6.2
5	59.4	5	13.0
6	47.1	6	15.9
7	12.0	7	56.9
8	-8.7	8	-7.8
9	84.3	9	85.8
10	52.0	10	2.0
11	74.3	11	-10.4
12	55.5	12	-16.3
13			nearly cloudless
14	185.5	13	5.0
15	58.3	14	40.1
16	102.2	15	50.7
17	14.2	16	2.7
18		17	-10.5
19		18	10.6
20	-10.1	19	
21	-10.5	20	28.5
22	38.5	21	-44.2
23	-2.0	22	-6.3
24	11.0	23	34.0
25	-6.4	24	26.6
	nearly cloudless	25	31.6
26	-7.1	26	22.3
	nearly cloudless	27	-8.7
27	-10.5	28	-22.5
	nearly cloudless	29	-17.0
28	10.2		nearly cloudless
29	-5.8	30	3.8
30	29.2	31	36.3

August		August	
1	8.5	20	-10.3
2	-0.9	21	23.4
3	-28.0	22	-4.5
4	-3.0		nearly cloudless
5	53.7	23	118.5
6	69.5	24	2.2
7	31.9	25	-8.7
8	42.8	26	5.1
9	5.1	27	-1.4
10	2.2	28	11.3
11	-13.6	29	18.2
12	56.3	30	15.7
13	6.2	31	-12.7
14			
15	0.9		
16			
17	-34.6		
18	-21.7		
19	-10.5		

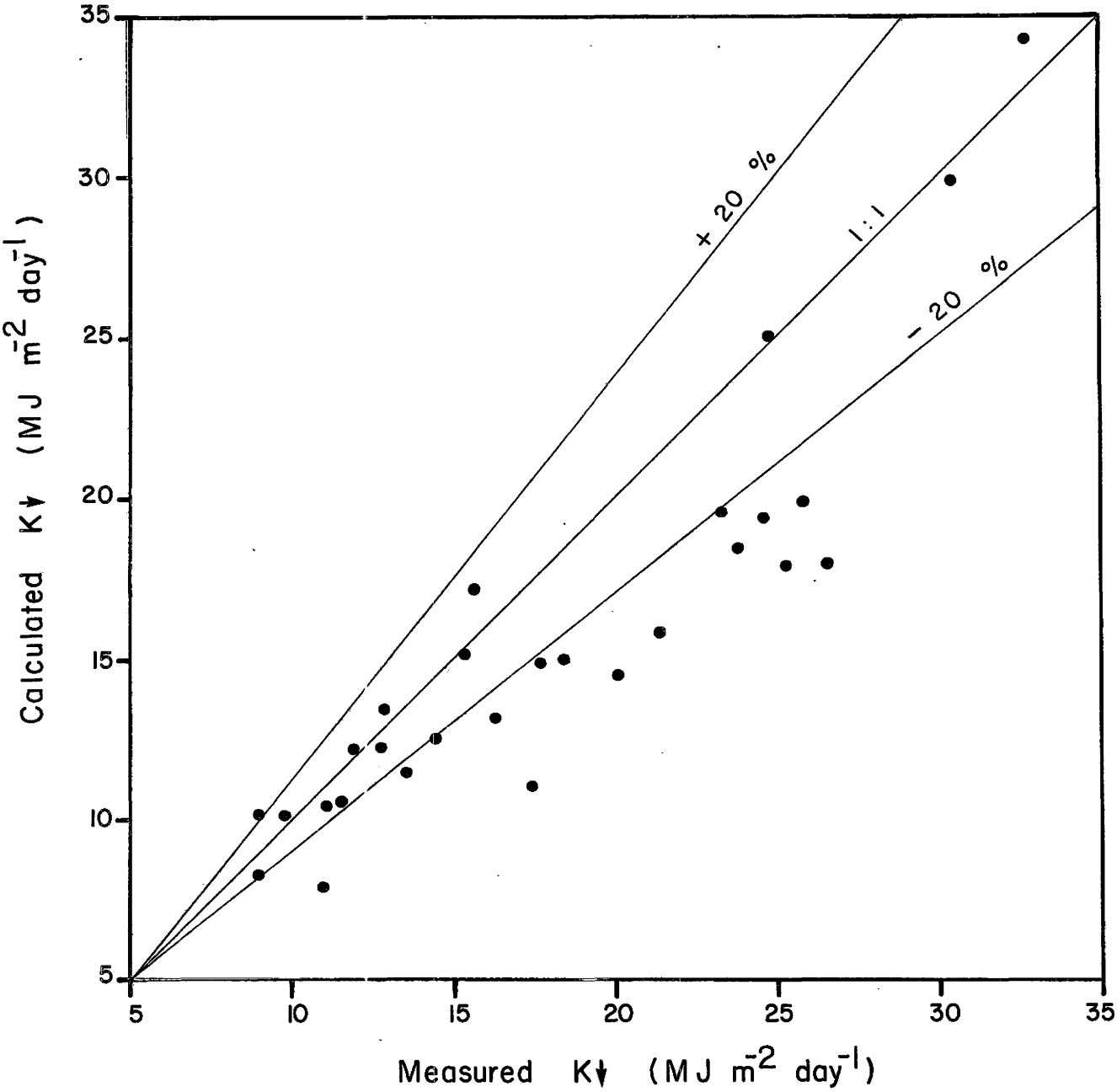

Figure 13: Correlation of measured and calculated solar radiation (K↓) for five day mean periods.

TABLE 11

Comparison of five day mean measured and calculated solar radiation values.

Date	Measured $K\downarrow$ ($MJm^{-2}day^{-1}$)	Calculated $K\downarrow$ ($MJm^{-2}day^{-1}$)	Measured-Calculated % difference
4/1-4/5/74	9.939	10.234	-3
4/6-4/10/74	12.003	12.322	-3
4/11-4/16/74	13.578	13.466	1
4/17-4/22/74	14.582	12.597	16
4/23-4/28/74	17.715	14.802	20
4/29-5/5/74	18.528	15.058	23
5/6-5/10/74	17.581	11.138	58
5/11-5/15/74	20.211	14.505	39
5/16-5/20/74	23.453	19.564	20
5/21-5/27/74	23.863	18.306	30
5/28-6/1/74	25.806	19.814	30
6/2-6/6/74	25.379	17.787	43
6/7-6/11/74	24.726	19.384	28
6/12-6/17/74	26.644	17.913	49
6/20-6/24/74	30.405	19.901	2
6/25-6/29/74	32.814	34.343	-4
6/30-7/4/74	21.543	15.779	37
7/5-7/9/74	16.375	13.188	24
7/10-7/14/74	24.919	25.045	-1
7/15-7/20/74	13.619	11.451	19
7/21-7/25/74	11.601	10.606	9
7/26-7/30/74	15.873	17.234	-8
7/31-8/4/74	15.437	15.156	2
8/5-8/9/74	11.098	8.015	38
8/10-8/15/74	9.096	8.417	8
8/16-8/21/74	9.155	10.225	-10
8/22-8/26/74	12.782	12.344	4
8/27-8/31/74	11.174	10.531	6

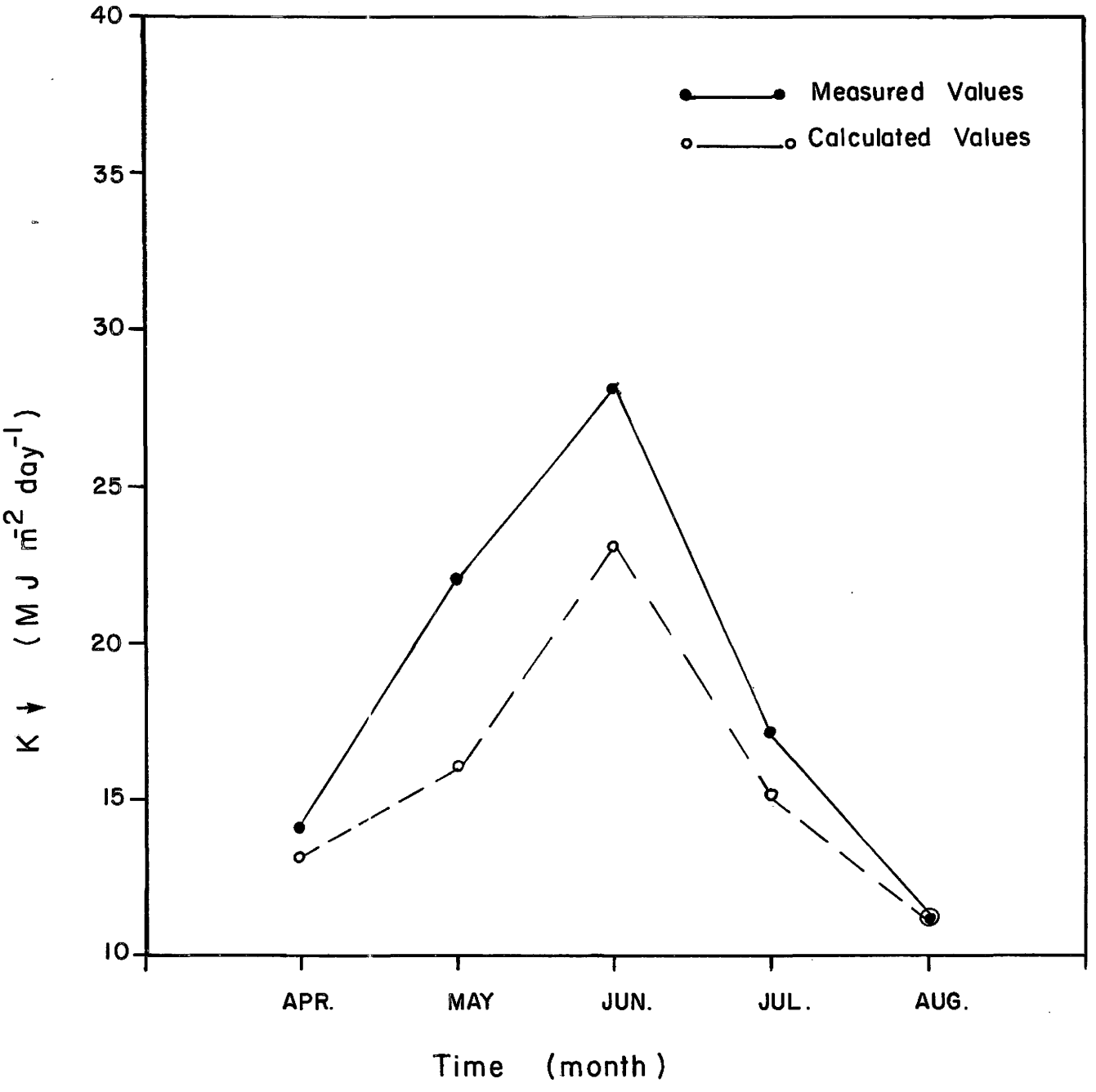

Figure 14 : Comparision of measured and calculated solar radiation (K ↓) for monthly periods

TABLE 12

Comparison of mean monthly measured and calculated solar radiation ($K\downarrow$) at Resolute.

	Measured $K\downarrow$ ($MJm^{-2}day^{-1}$)	Calculated $K\downarrow$ ($MJm^{-2}day^{-1}$)	Measured-Calculated % difference
April	13.930	12.968	7.4
May	21.756	16.443	32.3
June	27.732	23.399	18.5
July	16.943	15.245	11.1
August	11.343	10.782	5.2

and 14 (Table 12) indicate closer agreement to within ± 20% on about 16% and 80% respectively of the mean measured values.

On a daily basis, Figure 12 and Table 10 indicate that largest differences between computed and observed values are correlated with greatest cloud cover. In order to assess the influence of clouds on solar transmissions two sets of very contrasting days, (those with maximum cloud cover with persistent precipitation activity and those with varied cloud cover with minimal precipitation activity), are examined (Tables 13, 14).

(F) Analysis of Model Performance with Weather Conditions

The overall model performance is judged to be poor (Figure 12). However, a closer lock at weather conditions may provide some insight for daily variations; being days when solar radiation sensor records are either missing, incomplete or interpolated (indicated in Table 13 as E). A.E.S. daily surface records indicate 57 days of persistent precipitation activity. For these days, (Table 13) a large correlation exists between periods of precipitation activity and consistent model underestimation of observed values, irrespective of the precipitation form (ie. frozen or liquid).

Although precipitation activity by itself should have little effect on model performance, it does have other implications. For those days severely affected by precipitation activity, A.E.S. daily surface records also indicate, for 50 of the 57 days, the presence of fog and observer obstructions other than fog persisting for 5 hours or longer (indicated in Table 13 as OV). The combination of these two factors can be expected to affect the observers' perspective of cloud amounts at low and higher levels,

TABLE 13

Comparison of daily measured and calculated solar radiation with surface weather conditions

Date	Measured $K\downarrow$ ($MJm^{-2}day^{-1}$) (E indicates days where 1 or more hours are estimated)	Calculated $K\downarrow$ ($MJm^{-2}day^{-1}$)	Measured-calculated % difference	Mean daily cloud amount	Precipitation activity and surface observed obstructions to Vision(OV) FP=frozen precipitation LP=liquid precipitation 1=0 to 5 hrs occurance 2=5 to 10 hrs occurance 3=more than 10 hrs occurance
4/3/74	9.926E	11.797	-15.9	.64	FP-3/OV-1
4/5/74	9.130	8.147	12.1	.98	FP-3/OV-3
4/6/74	11.391	11.181	1.9	.51	FP-1/OV-3
4/7/74	11.894	11.719	1.5	.15	FP-1/OV-3
4/11/74	11.685E	12.455	-6.2	.28	FP-2/OV-3
4/12/74	14.742E	13.496	9.2	.12	FP-1/OV-2
4/13/74	13.779E	14.001	-1.5	.61	OV-2
4/14/74					
4/16/74	13.318	12.798	4.1	.85	FP-3/OV-3
4/19/74	14.155	11.343	24.8	.76	FP-3/OV-3
4/20/74					
4/21/74	11.098	6.863	61.7	.99	FP-3/OV-3
4/23/74	15.621	11.540	35.4	.81	FP-3/OV-3
4/24/74	18.888E	15.797	19.6	.51	FP-3/OV-1
4/26/74					
4/27/74	15.705E	10.705	46.7	.82	FP-3/OV-3
5/1/74	18.720E	14.154	32.3	.64	FP-2
5/2/74	18.092	14.843	21.9	.75	FP-1/OV-2
5/3/74					
5/4/74					
5/5/74	18.804	13.247	41.9	.93	FP-3/OV-3
5/6/74	19.307	12.855	50.1	.66	FP-3/OV-3
5/7/74	21.233	18.467	15.0	.75	OV-3
5/8/74	16.878	9.088	85.7	.95	FP-3
5/9/74	15.328	9.095	68.5	1.0	FP-3/OV-2
5/10/74	15.161E	6.182	145.2	1.0	FP-3/OV-3
5/11/74	16.249	9.574	69.7	1.0	FP-3/OV-3
5/12/74	18.637	7.519	147.8	1.0	FP-3/OV-3
5/13/74	17.925E	8.993	90.4	.83	FP-2/OV-2
5/14/74	22.070E	18.439	19.7	.47	
5/18/74	22.448	16.172	38.8	.96	FP-3
5/19/74	20.019	12.612	58.7	.95	FP-3/OV-2
5/20/74	23.997	18.056	32.9	.78	FP-3/OV-1
5/21/74	21.819	16.173	34.9	.94	FP-3/OV-2

Table 13 continued ....

5/22/74	23.118	13.913	66.2	.96	FP-3/OV-3
5/23/74					
5/24/74	23.160	12.777	81.3	.91	FP-3
5/25/74	27.850	30.023	-7.2	.23	FP-1
5/26/74					
5/27/74	23.369	18.642	25.4	.86	FP-2/OV-1
5/28/74	22.699	13.651	66.3	.90	FP-3
5/29/74	25.337	19.573	29.4	.71	FP-3/OV-2
5/30/74	28.813E	25.798	11.7	.88	FP-3
5/31/74	29.400E	25.127	17.0	.89	FP-3
6/1/74	22.783	15.057	51.3	.95	FP-3/OV-3
6/2/74	23.034	16.046	43.5	.93	FP-3
6/3/74	29.190	23.161	26.0	.81	FP-3/OV-1
6/4/74	27.766	19.082	45.5	.78	FP-3/OV-2
6/5/74	23.578	14.792	59.4	.83	FP-3/OV-2
6/6/74	23.327E	15.856	47.1	.89	FP-3/OV-3
6/7/74	31.661E	28.257	12.0	.37	FP-3
6/8/74	29.107	31.892	-8.7	.41	
6/9/74	23.327	12.655	84.3	.94	LP-3/FP-1
6/10/74	17.087	11.239	52.0	1.0	LP-1/FP-2/OV-3
6/11/74	22.448	12.878	74.3	.99	LP-1/FP-3
6/12/74	23.788E	15.291	55.5	.99	FP-3/OV-1
6/13/74					
6/14/74	29.944	18.488	62.0	.71	FP-1
6/15/74	23.160	14.626	58.3	.84	FP-1/OV-2
6/16/74	21.443	10.604	102.2	.95	LP-2/FP-2/OV-2
6/17/74	34.886	30.560	14.2	.27	
6/18/74					
6/19/74					
7/1/74	18.385	9.859	86.5	1.0	LP-1/FP-3/OV-1
7/2/74	24.751	15.223	62.6	.83	LP-2/FP-1/OV-2
7/6/74	15.454	13.337	15.9	.96	LP-2/OV-3
7/7/74	20.270	12.922	56.9	.93	LP-3/OV-3
7/9/74	20.228	10.885	85.8	.90	OV-3
7/17/74	7.622	8.515	-10.5	1.0	LP-3/OV-3
7/19/74					
7/20/74	18.595E	14.475	28.5	.90	OV-3
7/21/74	5.486	9.829	-44.2	.99	OV-3
7/22/74	9.800	10.464	-6.3	.93	LP-3/FP-3
7/24/74	15.998	12.633	26.6	.89	LP-1/FP-2/OV-1
7/27/74	22.113	22.214	-8.7	.59	
7/28/74	12.773	16.483	-22.5	.81	

Table 13 continued .....

8/6/74	11.978	7.067	69.5	.96	LP-2/OV-3
8/7/74	8.669	6.572	31.9	.96	LP-2/OV-3
8/8/74	9.004	6.305	42.8	.98	LP-1/OV-3
8/14/74					
8/15/74	6.910	6.848	0.9	.97	LP-2/FP-3
8/16/74					
8/17/74	4.481	6.853	-34.6	.96	LP-2/FP-3/OV-1
8/18/74	8.334	10.640	-21.7	.81	LP-2
8/19/74	7.832	8.748	-10.5	.86	OV-2
8/20/74	14.867E	16.571	-10.3	.65	OV-2
8/21/74	10.261	8.316	23.4	.53	OV-3
8/23/74	6.282	2.875	118.5	.99	LP-3/OV-3

and therefore, may severely limit cloud layer correction procedures.

For the 65 days where minimal or no precipitation activity was recorded by A.E.S. (Table 14), eight of which being affected by fog and observer obstructions other than fog, closer agreement between calculated and observed daily values is indicated (Figure 15). In 90% of the cases calculated values agree to within $\pm$ 20% of measured values (70% within $\pm$ 15% and 48% within $\pm$ 10%).

(G) Hourly Analysis of Model Performance

The influence of increasing cloud amount on model performance was evaluated for hourly periods on days of minimal or no precipitation activity (Table 15). The hourly values are plotted for typical days of nearly cloudless ($c < 4/10$) and cloudy sky ($c \rightarrow 10/10$) conditions (Figures 16A, B, C, D and 16E, F, G, H). At large zenith angles, both sets exhibit a tendency to underestimate measured values. In these instances, it may be that the surface albedo values that were used are inappropriate or that the model underestimated the multiply reflected contribution to the surface flux for zenith angles ($\geq 80^{o}$) characteristic of this time of day.

At smaller zenith angles, the comparison of measured to observed values for cloud amount less than 4/10 indicates consistent model overestimates (Figure 16A, B, C, D). With increased cloud amount, varying degree of model underestimation is observed (Figure 16E, F, G, H).

(H) Evaluation of Model Underestimation

Since meteorological data for Resolute showed the presence of snow cover up until the middle of June, a correlation between periods of

TABLE 14

Comparison of measured and computed solar radiation values for days of no or minimal precipitation activity

Date	Measured $K\downarrow$ ($MJm^{-2}day^{-1}$)	Calculated $K\downarrow$ ($MJm^{-2}day^{-1}$)	Measured-Calculated % difference	Mean daily cloud amount
4/1/74	9.591	10.002	-4.1	.02
4/2/74	10.117	10.266	-1.5	.29
4/4/74	10.931	10.958	-0.2	.25
4/8/74	12.187	11.830	3.0	.23
4/9/74	12.396	13.618	-9.0	.38
4/10/74	12/145	13.260	-8.4	.33
4/15/74	14.365	14.582	-1.5	.18
4/17/74	15.579	14.331	8.7	.46
4/18/74	14.658	14.371	2.0	.63
4/22/74	17.422	16.079	8.3	.51
4/25/74	19.181	17.476	9.7	.46
4/28/74	19.181	18.487	3.7	.45
4/29/74	17.338	15.576	11.3	.81
4/30/74	19.684	17.470	12.7	.56
5/15/74	26.175	27.999	-6.5	.07
5/16/74	25.463	26.288	-3.1	.25
5/17/74	25.337	24.693	2.6	.40
6/20/74	32.750	36.445	-10.1	.52
6/21/74	31.829	35.567	-10.5	.49
6/22/74	27.431	19.801	38.5	.93
6/23/74	30.363	30.974	-1.9	.79
6/24/74	29.651	26.718	11.0	.55
6/25/74	33.127	35.386	-6.4	.10
6/26/74	33.127	35.662	-7.1	.02
6/27/74	32.913	26.765	-10.5	.06
6/28/74	33.127	30.065	10.2	.38
6/29/74	31.871	33.835	-5.8	.32
6/30/74	26.049	20.158	29.2	.67
7/3/74	21.443	17.566	22.1	.95
7/4/74	17.087	16.090	6.2	1.0
7/5/74	10.386	11.938	13.0	.98
7/8/74	15.537	16.858	-7.8	.84
7/10/74	27.892	27.343	2.0	.43
7/11/74	27.934	31.191	-10.4	.43
7/12/74	27.180	32.455	-16.3	.29
7/13/74	19.139	18.219	5.0	.93
7/14/74	22.448	16.019	40.1	.89
7/15/74	18.595	12.338	50.7	.89
7/16/74	12.606	12.271	2.7	.95
7/18/74	10.679	9.655	10.6	.92
7/23/74	14.072	10.500	34.0	.93

Table 14 continued ....

7/25/74	12.648	9.605	31.6	.94
7/26/74	14.700	12.024	22.3	.87
7/29/74	20.731	24.978	-17.0	.45
7/30/74	9.046	8.719	3.8	.95
7/31/74.	14.700	10.758	36.6	.87
8/1/74	21.275	19.604	8.5	.59
8/2/74	14.700	14.846	-0.9	.92
8/3/74	9.088	12.619	-27.9	.79
8/4/74	17.422	17.953	-3.0	.47
8/5/74	14.826	9.645	53.7	.59
8/9/74	11.014	10.475	5.1	.86
8/10/74	11.517	11.269	2.2	.85
8/11/74	7.915	9.158	-13.6	.95
8/12/74	10.638	6.806	56.3	.95
8/13/74	8.502	8.004	6.2	1.0
8/22/74	15.454	16.186	-4.5	.30
8/24/74	14.532	14.216	2.2	.33
8/25/74	14.909	16.322	-8.7	.01
8/26/74	12.732	12.119	5.1	.62
8/27/74	9.339	9.469	-1.4	.59
8/28/74	11.140	10.007	11.3	.55
8/29/74	12.690	10.729	18.3	.42
8/30/74	12.650	10.933	15.7	.37
8/31/74	10.051	11.515	-12.7	.66

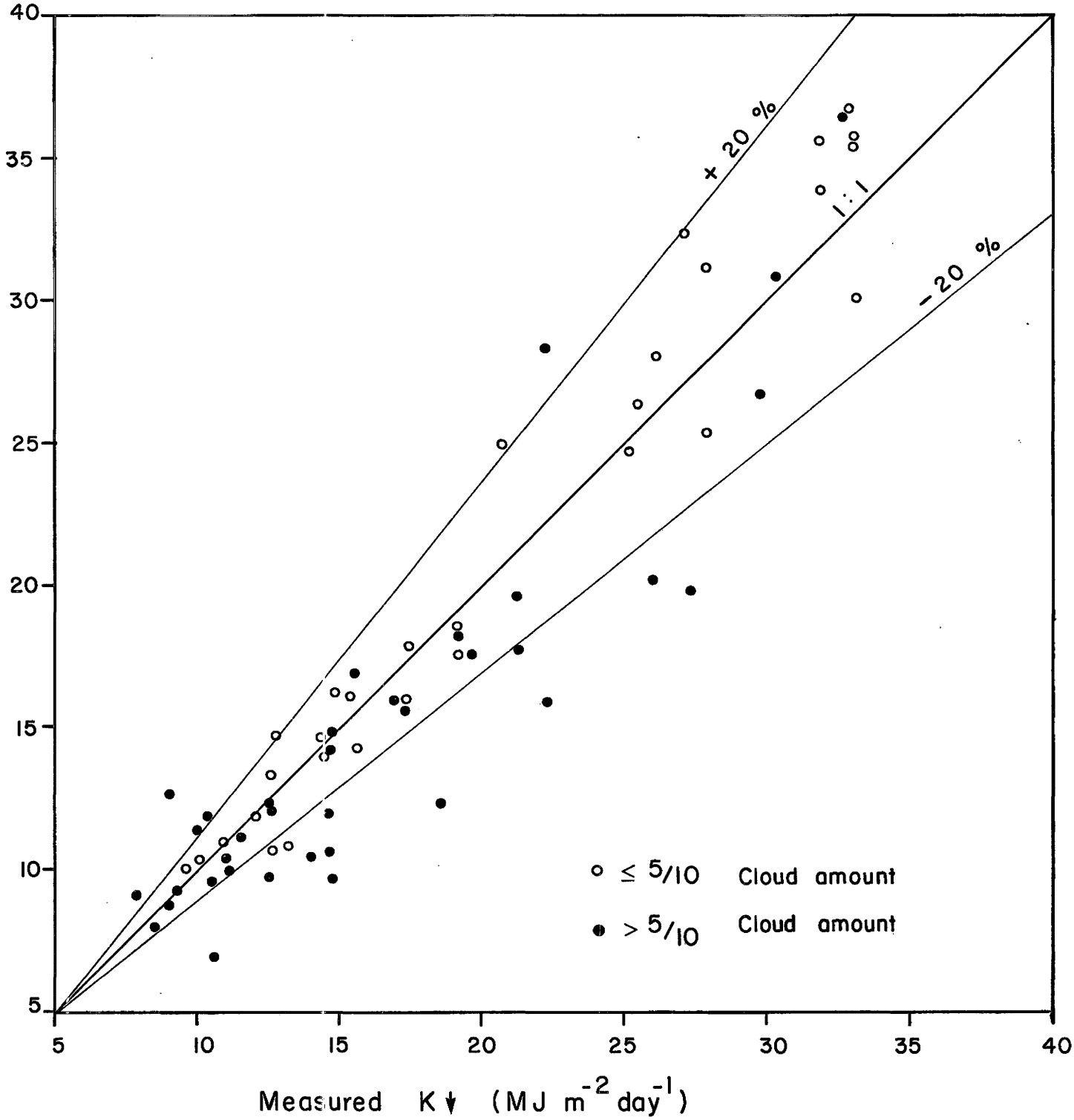

Figure 15 Correlation between measured and calculated daily values of solar radiation with cloud amount.

TABLE 15

Comparison of hourly measured and calculated solar radiation for cloudy and nearly cloudless days

Date	Time (LAT)	Measured $K\downarrow$ (Wm^{-2})	Calculated $K\downarrow$ (Wm^{-2})	Ratio measured to calculated	Mean cloud amount	Layer cloud amount	Layer cloud type
4/8/74	5	11.6	8.4	.7	.2	.2	Sc
	6	69.8	52.1	.7	.1	.1/.1	Sc/Ac
	7	139.6	110.2	.8	.4	.1/.1/.1	Sc/Ac/Ci
	8	209.4	189.3	.9	.2	.1/.1	Fg/Ac
	9	255.9	260.0	1.0	0.0	.1/.1	Fg/Ac
	10	225.7	318.0	1.0	.1	.1/.1	Fg/Ac
	11	395.5	336.1	.8	.3	.1/.2	Fg/Ac
	12	395.5	294.4	1.0	.2	.1/.1	Sc/Ci
	13	395.5	391.2	1.0	.2	.1/.1	Sc/Ci
	14	337.4	343.6	1.0	.2	.1/.1/.1	Sc/Ac/Ci
	15	337.4	317.8	.9	.2	.1/.1	Sc/Ci
	16	279.2	241.6	.9	0.0	.1/.1	Fg/Ac
	17	139.6	175.7	1.3	.2	.1/.2	Ac/Ci
	18	81.4	99.6	1.2	.3	.1/.3	Ac/Ci
	19	46.5	33.1	.7	.8	.1/.8	Ac/Ci
	20	23.3	2.4	.1	.2	.1/.2	Sc/Ci
4/29/74	2	11.6	1.7	.1	.3	.1/.3	Ac/Ac
	3	11.6	16.6	1.4	.2	.2/.1	Ac/Ac
	4	69.8	49.3	.7	.4	.1/.2/.1	Ac/Ac/Ci
	5	151.2	69.5	.5	.8	.1/.7	Ac/Ac
	6	116.3	148.1	1.3	.9	.4/.5	Ac/Cs
	7	186.1	178.4	1.0	.9	.1/.5/.4	Sc/Ac/Ci
	8	267.6	245.9	.9	1.0	.1/.9	Ac/Cs
	9	302.5	331.2	1.1	.9	.1/.9	Ac/Ci
	10	360.6	379.6	1.1	.9	.2/.8	As/Ci
	11	442.1	397.4	.9	.9	.3/.8	As/Ci
	12	500.2	428.0	.9	.9	.3/.7	As/Ci
	13	511.9	418.1	.8	.8	.1/.1/.7	Sc/Ac/Ci
	14	453.7	381.0	.8	.9	.1/.1/.8	Sc/Ac/Ci
	15	360.6	352.7	1.0	.9	.1/.9	Sc/Ci
	16	349.0	298.6	.9	.9	.1/.1/.8	Sc/Ac/Ci

4/29/74	17	255.9	242.6	.9	.9	.1/.1/.8	Sc/Ac/Ci
	18	174.5	182.0	1.0	.9	.1/.1/.8	Sc/Ac/Ci
	19	139.6	120.4	.9	.9	.1/.1/.8	Fg/Ac/Ci
	20	69.8	48.2	.7	.9	.1/.7/.2	Fg/Ac/Ci
	21	46.5	20.2	.4	1.0	.1/.6/.4	Fg/Ac/Ci
	22	23.3	3.2	.1	.9	.1/.1/.7	Fg/Ac/Ci
6/22/74	1	104.7	61.8	.6	1.0	.1/.9	Ac/Cs
	2	139.6	102.8	.7	.9	.2/.8	Ac/Ci
	3	104.7	132.8	1.3	.9	.2/.8	Ac/Ci
	4	197.8	185.7	.9	.8	.4/.4	Ac/Ci
	5	279.2	212.3	.8	.9	.8/.1	Ac/Ci
	6	290.8	248.6	.9	.9	.9/.1	Ac/Ci
	7	430.4	314.3	.7	.9	.9	Ac
	8	395.5	335.5	.8	.9	.4/.5	Sc/Ac
	9	523.5	349.3	.7	.9	.4/.6	Sc/Ac
	10	477.0	356.5	.7	1.0	.6/.5	Sc/Ac
	11	477.0	277.9	.6	1.0	1.0/.1	Sc/Ac
	12	546.8	328.4	.6	1.0	.9/.2	Sc/Ac
	13	604.9	349.0	.6	.9	.9/.1	Sc/Ac
	14	488.6	358.0	.7	.9	.9	Sc
	15	488.6	369.2	.8	.9	.8/.1	Sc/Ac
	16	372.3	333.6	.9	.9	.8/.1	Sc/Ac
	17	372.3	309.3	.8	.9	.7/.2	Sc/Ac
	18	418.8	213.3	.5	.9	.8/.3	Sc/Ac
	19	255.9	168.4	.7	.9	.9/.1	Sc/Ac
	20	209.4	156.1	.7	.9	.2/.7	Sc/Ac
	21	139.6	84.1	.6	1.0	.1/1.0	Sf/Ac
	22	128.0	62.1	.5	1.0	.1/1.0	Sf/Ac
	23	116.3	78.2	.7	1.0	.5/.4/.1	Ac/As/Ci
	24	93.1	66.1	.7	1.0	.3/.7	Ac/Cs
6/29/74	1	81.4	76.7	.9	1.0	.1/.1/.9	St/As/Ci
	2	162.9	76.7	.5	1.0	.1/3./.7	Sf/Ci/Cs
	3	174.5	92.9	.5	1.0	.1/.2/.9	Sf/Ci/Cs
	4	197.8	142.3	.7	1.0	.1/.3/.7	Sf/Ci/Cs
	5	151.2	288.1	1.9	.2	.1/.1	Ac/Ci
	6	197.8	338.2	1.7	.2	.1/.1/.1	St/Ac/Ci
	7	407.2	364.6	.9	.4	.1/.3/.1	Sf/Ac/Ci
	8	477.0	525.9	1.1	.3	.3	Ac

Table 15 continued ...

Table 15 continued ....

6/29/74	9	546.8	618.5	1.1	.2	.2	Ac
	10	604.9	679.9	1.1	.2	.2	Ac
	11	639.8	687.2	1.1	.1	.1/.1	Sc/Ac
	12	663.1	706.5	1.1	.1	.1/.1	Sc/Ac
	13	674.7	703.9	1.0	.2	.1/.1	Sc/Ac
	14	639.8	685.2	1.1	.3	.1/.1	Ac/Ci
	15	604.9	667.1	1.1	.2	.2	Ac
	16	546.8	601.9	1.1	.2	.2	Ac
	17	477.0	452.0	.9	.2	.1/.2/.1	Cf/Ac/Ci
	18	418.8	389.3	.9	.2	.1/.2	Cf/Ac
	19	337.4	333.9	1.0	.1	.1/.1	Sc/Ac
	20	279.2	240.4	.9	.2	.1/.1/.2	Fg/Ac/Ci
	21	197.8	179.3	.9	.2	.1/.1/.2	Fg/Ac/Ci
	22	151.2	136.1	.9	.1	.1/.1/.1	Fg/Ac/Ci
	23	116.3	107.9	.9	.1	.1/.1	Fg/Ac
	24	104.7	93.3	.9	0.0	.1/.1	Fg/Ac
7/12/74	1	58.2	63.8	1.1	.9	.1/.1/.9	Ac/Ci/Cs
	2	58.2	74.6	1.3	.9	.1/.1/.9	Ac/Ac/Ci
	3	69.8	100.7	1.4	.9	.1/.1/.9	Ac/Ac/Ci
	4	116.3	142.5	1.2	.8	.1/.1/.8	Ac/Ac/Ci
	5	221.0	203.8	.9	.8	.1/.8	Ac/Ci
	6	279.2	319.7	1.1	.8	.8	Ci
	7	349.0	413.0	1.2	.5	.5	Ci
	8	418.8	505.3	1.2	.3	.3	Ci
	9	488.6	575.4	1.2	0.0	.1	Ac
	10	546.8	636.0	1.2	0.0	.1	Ac
	11	570.0	678.5	1.2	0.0	.1	Ac
	12	593.3	699.5	1.2	0.0	.1	Ac
	13	593.3	697.6	1.2	0.0	.1	Ac
	14	570.0	692.8	1.2	.1	.1	Ci
	15	535.1	646.0	1.2	.1	.1	Ci
	16	477.0	581.2	1.2	.1	.1	Ci
	17	418.8	497.4	1.2	.2	.2	Ci
	18	360.6	412.5	1.1	.2	.2	Ci
	19	279.2	328.1	1.2	.2	.2	Ci
	20	221.0	249.5	1.1	0.0	.1	Ci
	21	162.9	180.0	1.1	0.0	.1	Ci
	22	93.1	128.5	1.4	.3	.3	Ci
	23	58.2	95.4	1.6	.4	.4	Ci
	24	46.5	65.3	1.4	.8	.1/.8	Ac/Ci

Table 15 continued ....

7/14/74	1	58.2	19.3	.3	1.0	.2/.8	Sf/Ac
	2	46.5	15.2	.3	1.0	1.0	Fg
	3	81.4	46.0	.6	1.0	1.0	Sc
	4	81.4	113.1	1.4	.7	.2/.5	Sf/Ac
	5	162.9	87.3	.5	.9	.8/.2	Sf/Ac
	6	186.1	167.5	.9	.9	.1/.1/.1/.2	Sf/Sc/Sc/Ac
	7	244.3	170.0	.7	.9	.3/.1/.6/.1	Sc/Sc/Ac/Ac
	8	279.2	198.4	.7	.9	.1/.7/.3	Sf/Sc/Ac
	9	244.3	228.1	.9	.9	.1/.7/.3	Sc/Sc/Ac
	10	349.0	218.8	.6	.9	.1/.8/.3	Sc/Sc/Ci
	11	535.1	311.5	.6	.9	.3/.6/.2	Cf/Sc/Ac
	12	360.6	289.0	.8	.9	.5/.5/.2	Cf/Sc/Ci
	13	523.5	381.7	.7	.9	.6/.2/.1	Cf/Sc/Ac
	14	581.7	425.2	.7	.8	.4/.1/.1/.3	Cf/Sc/Ci/Ci
	15	558.4	373.4	.7	.9	.2/.4/.3	Cf/Sc/Ci
	16	546.8	314.5	.6	.8	.3/.4/.3	Cf/Sc/Ac
	17	407.2	343.7	.8	.9	.1/.1/.1/.6	Cf/Sc/Ci/Ci
	18	325.7	250.1	.8	.9	.2/.3/.5	Cf/Sc/Ci
	19	221.0	191.8	.9	.9	.3/.3/.4	Cf/Sc/Ci
	20	162.9	88.7	.5	.9	.7/.3/.1	Cf/Sc/Ci
	21	93.1	76.3	.8	.9	.4/.6/.1	Sc/Sc/Ci
	22	93.1	48.9	.5	.8	.8/.3	Sc/Sc
	23	69.8	32.2	.5	.9	.8/.4	Sc/Sc
	24	46.5	29.1	.6	.9	.9/.1	Sc/Sc
8/13/74	2	0.0	.7		1.0	.1/1.0	Cf/Sc
	3	11.6	4.2	.4	1.0	.1/.1/1.0	Cf/Sc
	4	23.3	15.1	.6	1.0	.1/1.0	Cf/Sc
	5	34.9	40.8	1.2	1.0	.1/.5/.5	Cf/Sf/Sc
	6	46.5	62.4	1.3	1.0	.1/.1/.5	Sf/Cf/Sc
	7	58.2	98.1	1.7	1.0	.1/.5/.5	Sf/Sf/Sc
	8	104/7	114.5	1.1	1.0	.1/.1/.9	Sf/Sc/Sc
	9	162.9	149.0	.9	1.0	.1/.9	Sf/Sc
	10	128.0	170.2	1.3	1.0	.1/.9	Sf/Sc
	11	232.7	187.8	.8	1.0	.8/.2	Sf/Sc
	12	290.8	233.2	.8	1.0	.6/.4	Sf/Sc
	13	267.6	213.5	.8	1.0	.2/.8	Sf/Sc
	14	197.8	209.3	1.1	1.0	.2/.8	Cf/Sc
	15	139.6	190.9	1.4	1.0	.2/.8	Cf/Sc
	16	267.6	165.4	.6	1.0	.2/.6/.2	Sf/Sf
	17	128.0	126.0	1.0	1.0	.7/.3	Sf/Sf

Table 15 continued ....

8/13/74	18	162.9	109.5	.7	1.0	.4/.6	Sf/Sc
	19	58.2	83.3	1.4	1.0	.1/.2/.7	Sf/Sc/Cb
	20	34.9	38.0	1.1	1.0	.4/.4/.5	Sf/Sc/Ac
	21	23.3	12.6	.5	1.0	.1/.8/.1	Cf/Sf/Sc
	22	11.6	2.2	.2	1.0	.1/.9/.1	Cf/Sf/Sc
	23	0.0	.6		1.0	.2/.8	Fg/Sf
8/22/74	3	0.0	.2		.3	.3	Ac
	4	11.6	7.7	.7	.9	.1/.9	Sc/Ac
	5	58.2	30.1	.5	.9	.1/.9	Sc/Ac
	6	116.3	87.4	.8	.6	.1/.6	Sc/Ac
	7	186.1	151.9	.8	.5	.1/.5	Sc/Ac
	8	255.9	295.2	1.2	.1	.1	Sc
	9	314.1	368.3	1.2	.1	.1	Sc
	10	372.3	428.6	1.2		.1	Sc
	11	407.2	471.6	1.2		.1	Sc
	12	430.4	492.5	1.1		.1	Sc
	13	430.4	489.8	1.1		.1	Sc
	14	407.2	463.6	1.1		.1	Sc
	15	360.6	375.6	1.0	.1	.1/.1/.1	Cu/Sc/Ci
	16	314.1	291.6	.9	.4	.1/.1/.4	Cu/Sc/Ci
	17	255.9	280.6	1.1	.5	.5	Ci
	18	186.1	198.3	1.1	.6	.6	Ci
	19	116.3	123.1	1.1	.5	.5	Ci
	20	58.2	54.0	.9		.1/.1	Sc/Ci
	21	23.3	12.5	.5		.1/.1/.1	Sc/Ac/Ci

Ci to high

Ac to low

Sc to high

Fractus to low

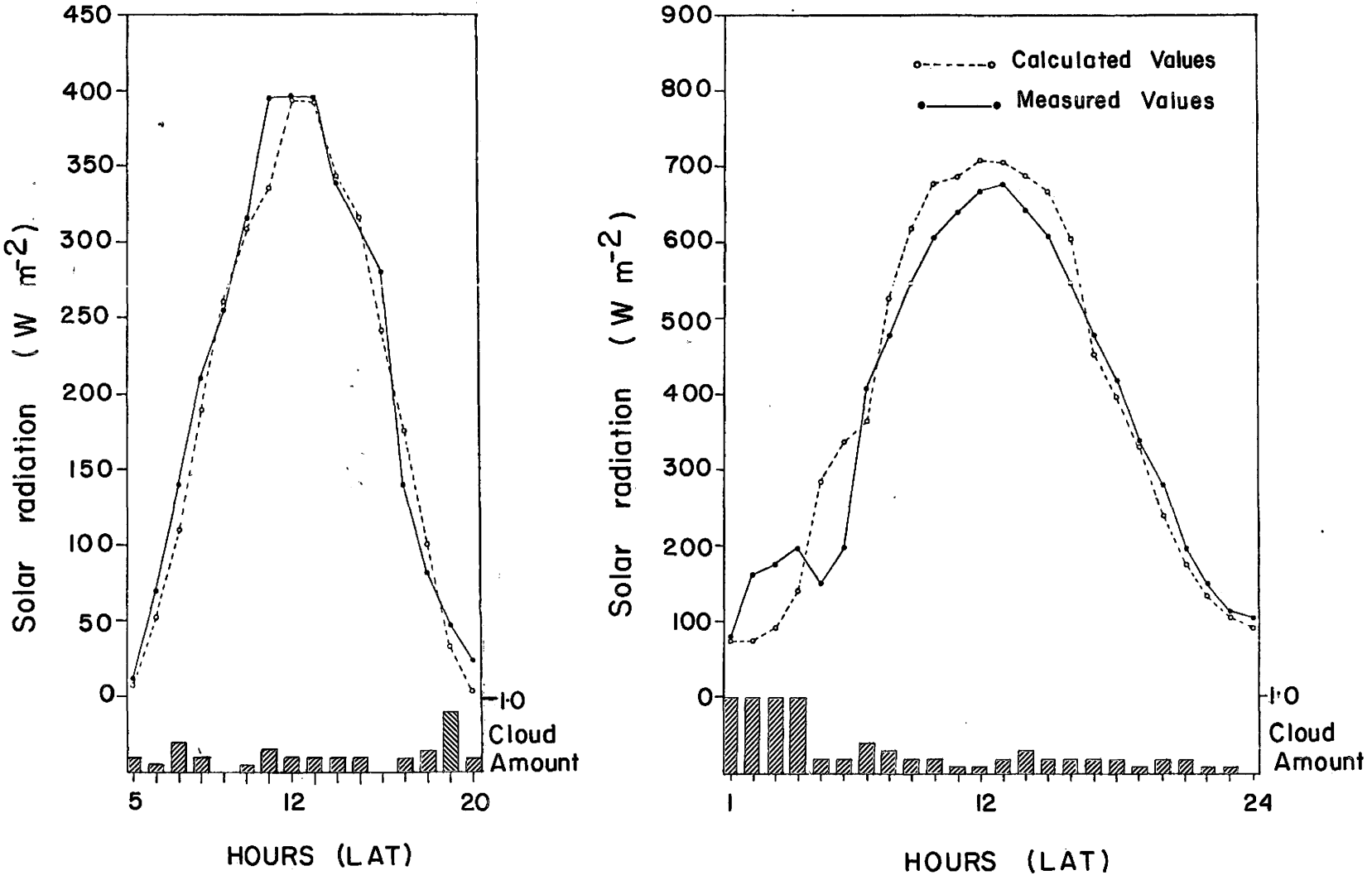

Figure : 16 Variations in hourly values of measured and calculated solar radiation (K↓) for nearly cloudless and cloudy days

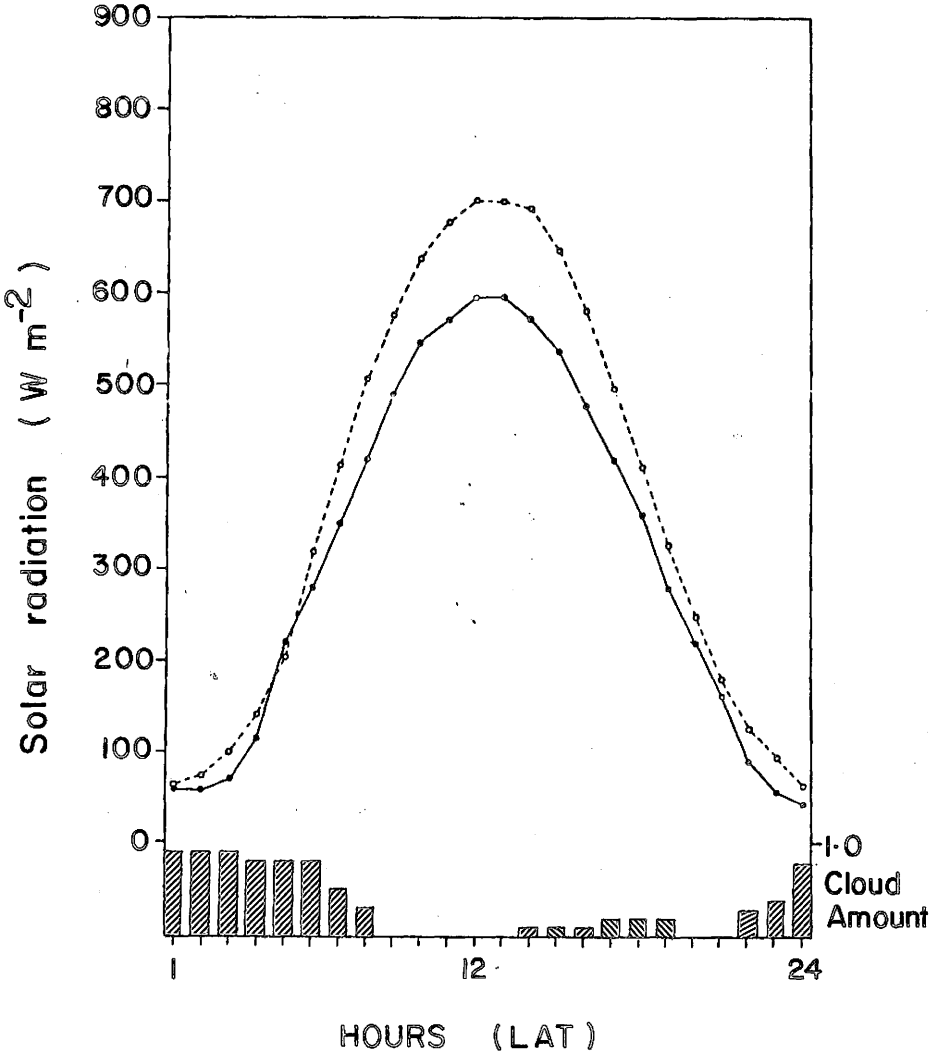

(C) July 12, 1974

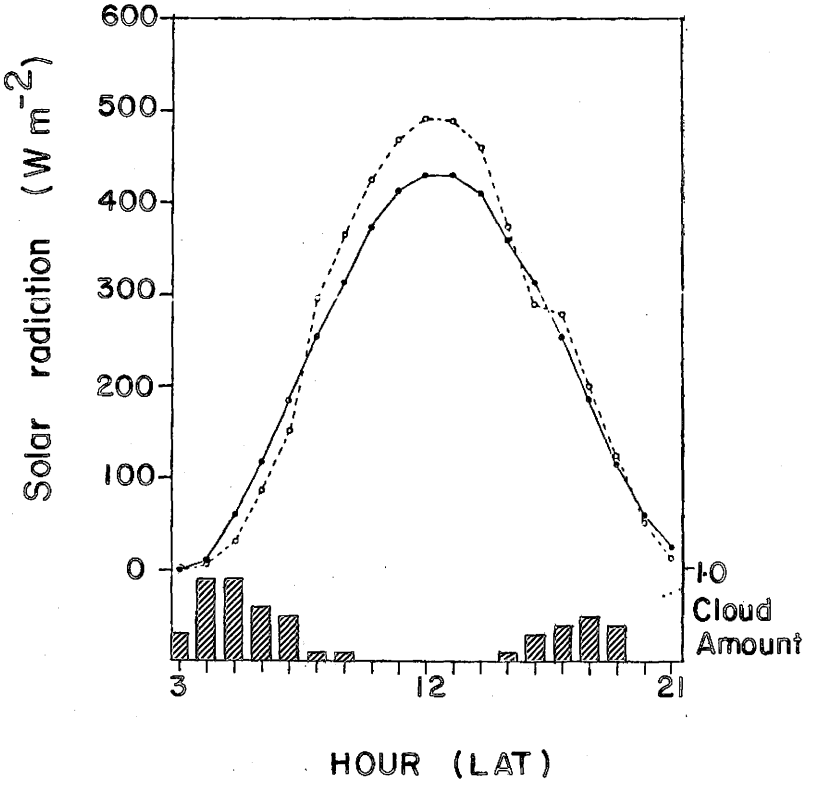

(D) August 22, 1974

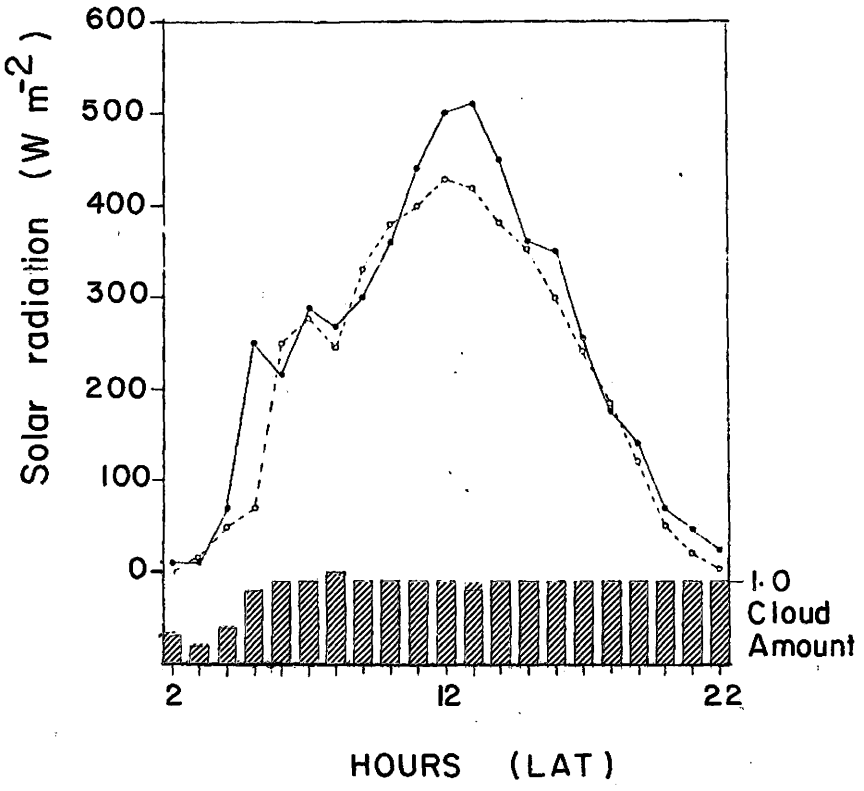

(E) April 29, 1974

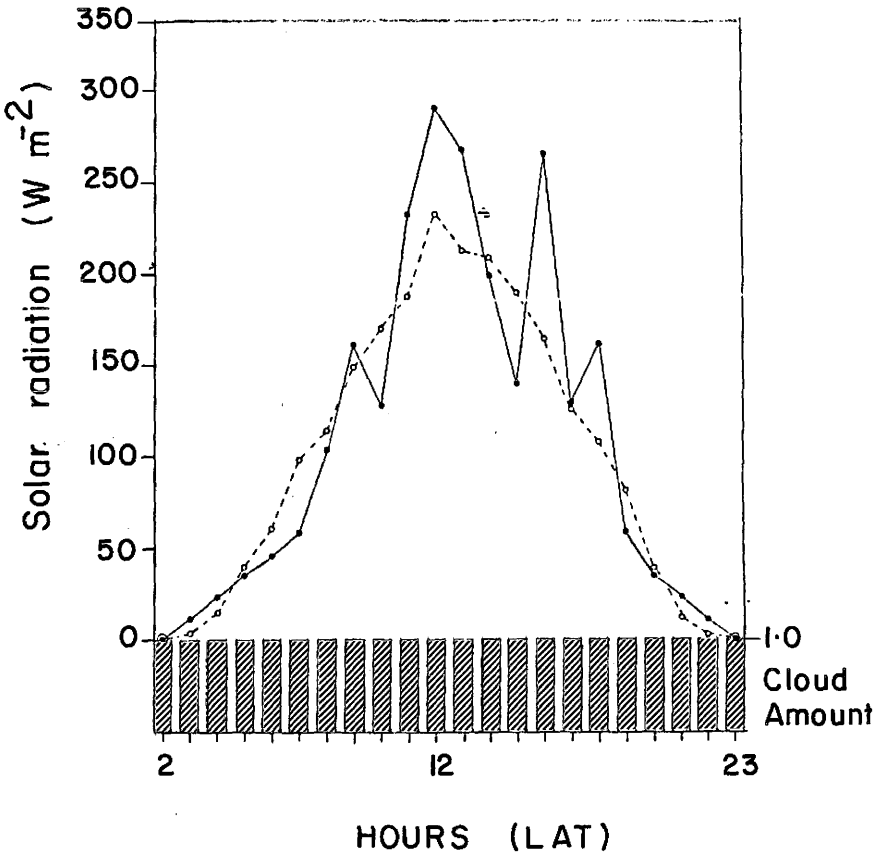

(F) August 13, 1974

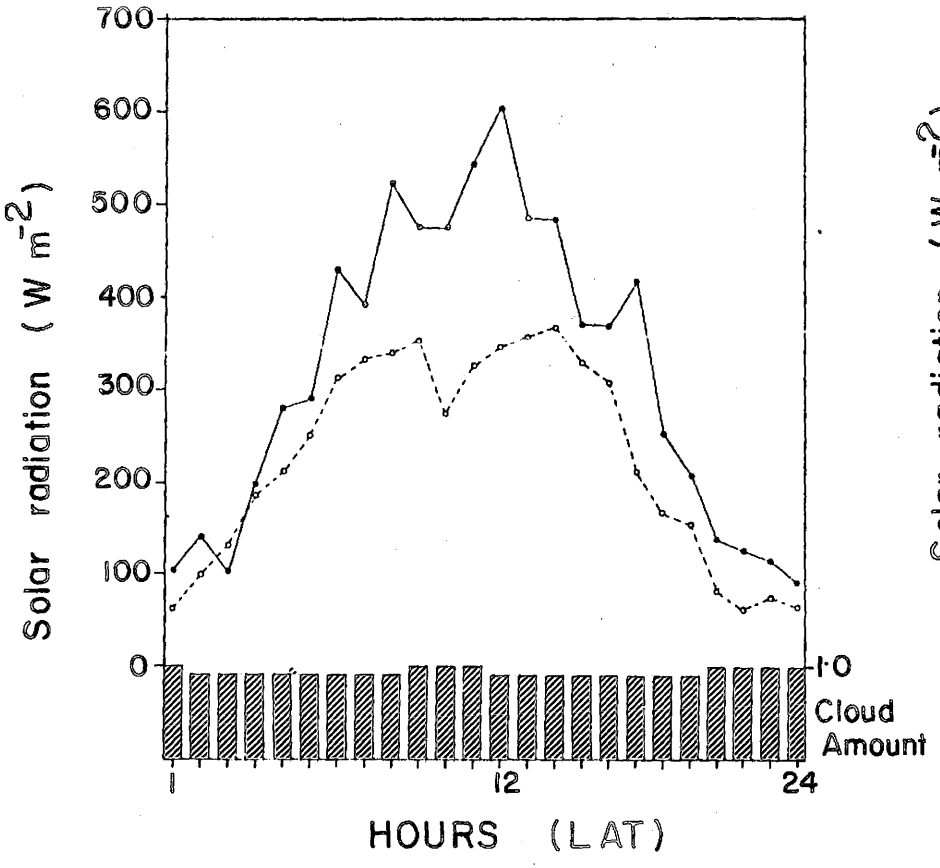

(G) June 22, 1974

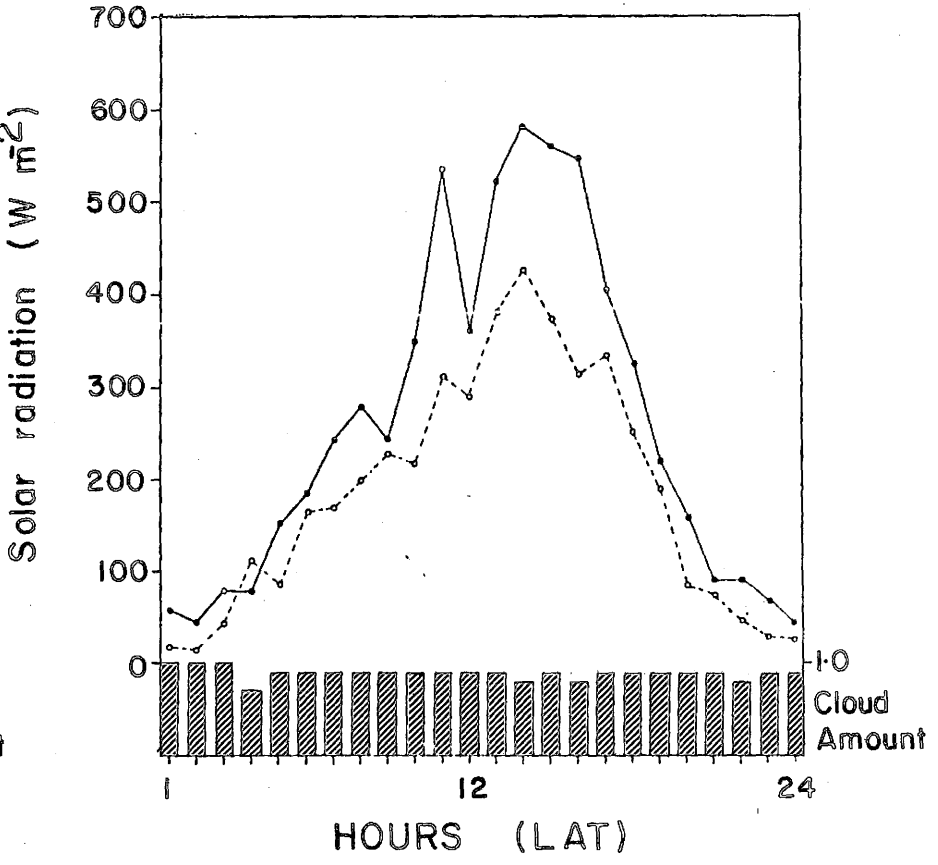

(H) July 14, 1974

snow cover and periods when computed radiation underestimated observed values may exist. During these periods, there is a high surface albedo and extensive cloud cover. As a result of high surface albedo, the downward flux associated with multiple reflections from middle and high cloud could increase daily values by up to 20% over previous results. This increase in the downward flux density should also be greater with the total cloud cover approaching unity in the presence of an incomplete low cloud layer.

Therefore, the reason for the model underestimation may result from the neglect of middle and high cloud reflected contributions.

Modifications to the procedure for computing the downward flux associated with the lowest cloud layer were made to express this flux as a function of the observed total cloud cover. This modified approach was evaluated on a daily basis for the full study period. A contrast of the two approaches is presented in Table 16.

As a result of using the total cloud cover reflections in calculating solar radiation received at the surface, Table 16 indicates that large model underestimation has been reduced for 42 of the 59 days of precipitation activity and observer obstructions to vision. However, the model tendency to underestimate observed daily values by more than 10% is indicated for 45 of those 59 days. For the days of no precipitation activity, indicated in Table 14, no improvement between measured and calculated values is observed using the total cloud cover reflection contribution to the surface flux. Furthermore, for these days there does not appear to be any correlation between mean daily cloud amount and improved model estimates.

Generally, for the 124 days considered, improved estimates of measured values are observed for about 56% of the days, with a dramatic modelling improvement being indicated for May and June, the period of major precipitation activity.

TABLE 16

Comparison of daily measured and calculated solar radiation values at Resolute for full study period using $K\downarrow_c(1-\alpha_c\,\alpha_g\,C_1)$ and $K\downarrow_c(1-\alpha_c\,\alpha_g\,C_T)$. (+ indicates days of precipitation activity and observer obstructions to vision).

Date	Measured $K\downarrow$ (Wm^{-2})	Calculated $K\downarrow$ using $(1-\alpha_c\,\alpha_g C_1)$ Wm^{-2}	Calculated $K\downarrow$ using $(1-\alpha_c\,\alpha_g C_1)$ Wm^{-2}	Measured-calculated % difference for $(1-\alpha_c\,\alpha_g C_1)$	Measured-calculated % difference for $(1-\alpha_c\,\alpha_g C_T)$
April					
1	9.591	10.002	9.636	-4.1	-0.4
2	10.117	10.266	10.364	-1.5	-2.4
3+	9.926	11.797	11.799	-15.9	-15.9
4	10.931	10.958	11.247	-0.2	-2.8
5+	9.130	8.147	10.862	12.1	-15.9
6+	11.391	11.181	12.660	1.9	-10.0
7+	11.894	11.719	11.956	1.5	-0.5
8	12.187	11.830	12.356	3.0	-1.4
9	12.396	13.618	13.552	-9.0	-8.5
10	12.145	13.260	13.717	-8.4	-11.1
11+	11.685	12.455	12.644	-6.2	-7.6
12+	14.742	13.496	13.854	9.2	6.4
13+	13.779	14.001	15.990	-1.5	-13.8
14					
15	14.365	14.582	15.334	-1.5	-6.3
16+	13.318	12.798	16.472	4.1	-19.1
17	15.579	14.331	16.061	8.7	-3.0
18	14.658	14.371	16.594	2.0	-11.7
19+	14.155	11.343	15.224	24.8	-7.0
20					
21+	11.098	6.863	9.400	61.7	18.0
22	17.422	16.079	18.401	8.3	-5.3
23+	15.651	11.540	15.806	35.4	-0.9
24+	18.888	15.797	18.191	19.6	3.8
25	19.181	17.476	19.394	9.7	-1.1
26					
27+	15.705	10.705	14.154	46.7	10.9
28	19.181	18.487	21.334	3.7	-10.1
29	17.338	15.576	21.455	11.3	-19.2
30	19.684	17.470	19.528	12.7	0.7
May					
1+	18.720	14.154	16.005	32.3	17.0
2+	18.092	14.843	17.582	21.9	2.9
3					
4					
5+	18.808	13.247	16.799	41.9	11.1
6+	19.307	12.855	15.568	50.1	24.0
7+	21.233	18.467	23.731	15.0	-10.5
8+	16.878	9.088	11.303	85.7	49.3

Table 16 continued ....

May					
9+	15.328	9.095	10.374	68.5	47.8
10+	15.161	6.182	7.421	145.2	104.3
11+	16.249	9.574	12.410	69.7	30.9
12+	18.637	7.519	8.749	147.8	113.0
13+	17.925	8.993	10.199	90.4	75.7
14+	22.070	18.439	19.960	19.7	10.6
15	26.175	27.999	26.700	-6.5	-2.0
16	25.463	26.288	25.991	-3.1	-2.0
17	25.337	24.693	25.175	2.6	0.6
18+	22.448	16.172	19.320	38.8	16.2
19+	20.019	12.612	15.299	58.7	30.9
20+	23.997	18.056	20.940	32.9	14.5
21+	21.819	16.173	19.482	34.9	12.0
22+	23.118	13.913	17.621	66.2	31.2
23					
24+	23.160	12.777	15.214	81.3	52.2
25+	27.850	30.023	29.538	-7.2	-5.7
26					
27+	23.369	18.642	22.190	25.4	5.3
28+	22.699	13.651	15.836	66.3	43.3
29+	25.337	19.573	22.146	29.4	14.4
30+	28.813	25.798	32.840	11.7	-12.2
31+	29.400	25.127	32.614	17.0	-9.9
June					
1+	22.783	15.057	17.983	51.3	26.7
2+	23.034	16.046	18.336	43.5	25.6
3+	29.190	23.161	25.620	26.0	13.9
4+	27.766	19.082	22.653	45.5	22.6
5+	23.578	14.792	15.887	59.4	48.4
6+	23.327	15.856	18.387	47.1	26.8
7+	31.661	28.257	28.550	12.0	10.9
8+	29.107	31.892	32.865	-8.7	-11.4
9+	23.327	12.655	13.076	84.3	78.4
10+	17.087	11.239	13.494	52.0	26.6
11+	22.448	12.878	16.170	74.3	38.8
12+	23.788	15.291	16.955	55.5	40.3
13					
14+	29.944	18.488	18.605	62.0	60.9
15+	23.160	14.626	16.794	58.3	37.9
16+	21.443	10.604	13.373	102.2	60.3
17+	34.886	30.560	30.189	14.2	10.5
18					
19					
20	32.750	36.445	37.251	-10.1	-12.1
21	31.829	35.567	36.991	-10.5	-13.9
22	27.431	19.801	21.531	38.5	27.4
23	30.363	30.974	34.119	-1.9	-11.0
24	29.651	26.718	28.470	11.0	4.1
25	33.127	35.386	34.486	-6.4	-3.9
26	33.127	35.662	34.683	-7.1	-4.5
27	32.918	36.765	35.951	-10.5	-8.4
28	33.127	30.065	32.548	10.2	1.7
29	31.871	33.835	35.081	-5.8	-9.2
30	26.049	20.158	22.595	29.2	15.2

Table 16 continued .....

July					
1+	18.385	9.859	10.695	86.5	71.9
2+	24.751	15.223	16.597	67.2	49.1
3	21.443	17.566	19.373	22.1	10.6
4	17.087	16.090	17.664	6.2	-3.3
5	10.386	11.938	13.328	13.0	-22.1
6+	15.454	13.337	15.572	15.9	-0.7
7+	20.270	12.922	15.112	56.9	34.1
8	15.537	16.858	18.326	-7.8	-15.2
9+	20.228	10.885	12.579	85.8	60.8
10	27.892	27.343	29.368	2.0	-5.0
11	27.934	39.191	31.929	-10.4	-12.5
12	27.180	32.455	32.534	-16.3	-16.5
13	19.139	18.219	20.559	5.0	-6.9
14	22.448	16.019	17.804	40.1	26.1
15	18.595	12.338	13.229	50.7	40.6
16	12.606	12.271	14.181	2.7	-11.1
17+	7.622	8.515	9.913	-10.5	-23.1
18	10.679	9.655	11.225	10.6	-4.9
19					
20+	18.595	14.475	15.887	28.5	17.0
21+	5.486	9.829	10.790	-44.2	-49.2
22+	9.800	10.464	11.782	-6.3	-16.8
23	14.017	10.500	10.787	34.0	29.9
24+	15.998	12.633	14.214	26.6	12.6
25	12.648	9.605	10.901	31.6	16.0
26	14.700	12.024	12.420	22.3	18.4
27+	22.113	24.214	25.294	-8.7	-12.6
28+	12.773	16.483	17.007	-22.5	-24.9
29	20.731	24.978	25.012	-17.0	-17.1
30	9.046	8.719	10.210	3.8	-11.4
31	14.700	10.758	11.505	36.6	27.7
August					
1	21.275	19.604	19.971	8.5	6.5
2	14.700	14.846	15.869	-0.9	-7.4
3	9.088	12.619	13.915	-27.9	-34.7
4	17.422	17.953	18.953	-3.0	-8.1
5	14.826	9.645	10.389	53.7	42.7
6+	11.978	7.067	8.142	69.5	47.1
7+	8.669	6.572	7.845	31.9	10.5
8+	9.004	6.305	7.515	42.8	19.8
9	11.014	10.475	11.697	5.1	-5.8
10	11.517	11.269	11.920	2.2	-3.4
11	7.915	9.158	10.697	-13.6	-26.0
12	10.638	6.806	7.084	56.3	50.2
13	8.502	8.004	9.131	6.2	-6.9
14					
15+	6.910	6.848	7.490	0.9	-7.7
16					
17+	4.481	6.853	7.003	-34.6	-36.0
18+	8.334	10.640	12.089	-21.7	-31.1
19+	7.832	8.748	9.837	-10.5	-20.4
20+	14.867	16.571	16.845	-10.3	-11.7

Table 16 continued ....

August					
21+	10.261	8.316	8.316	23.4	23.4
22	15.454	16.186	16.174	-4.5	-4.4
23+	6.282	2.875	4.320	118.5	35.9
24	14.532	14.216	14.205	2.2	2.3
25	14.909	16.322	16.151	-8.7	-7.7
26	12.732	12.119	13.538	5.1	-5.9
27	9.339	9.469	9.833	-1.4	-5.0
28	11.140	10.007	10.620	11.3	4.9
29	12.690	10.729	11.488	18.3	10.5
30	12.650	10.933	10.993	15.7	15.1
31	10.051	11.515	12.113	-12.7	-17.0

(I) DISCUSSION

From this study, which encompasses a variety of meteorological conditions, it is evident that the modelling of solar radiation response to cloud effects is not simple. When modelling the attenuation of solar radiation by clouds a number of problems arise. Firstly, observed cloud data can be expected to decrease in accuracy as cloud amount increases, especially in the presence of observer obstructions to vision such as fog and precipitation activity. Observer inability to accurately specify cloud amount above a complete or broken overcast at low to middle levels can lead to varying degrees of model over and underestimation. Under broken cloud conditions cloud overestimation for higher levels leads to model underestimation while under complete low layer overcast probable cloud amount underestimation results in model overestimation of observed values. Secondly, observed cloud data do not contain information needed to determine actual reflection, absorption and transmission characteristics of clouds. For instance, Liou (1976) demonstrated the strong influence of cloud location on solar absorption within a cloud layer (Figure 17) and the degree to which cloud reflection was inflenced by geometrical cloud depth (Figure 18). Although the model takes account of reflection occuring between the surface and cloud bases it does not consider the diffuse flux incident at the surface resulting from inter-cloud reflections. In these instances, due to the large zenith angles characteristic of Arctic areas, large model underestimates of the surface diffuse flux can be expected to occur.

Thirdly, the cloud transmission constants used in this study may not be representative of those experienced in the Resolute area. Haurwitz's (1948) analysis of transmission constants applied to conditions of complete overcast with one predominant cloud type. Although these constants have been used

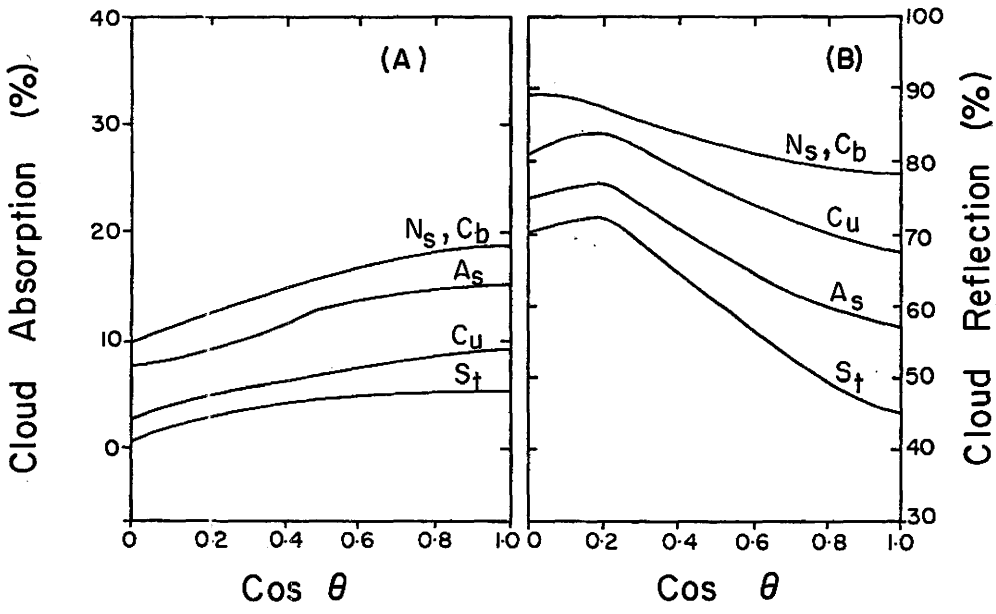

Figure: 17 Absorption (A) and reflection (B) of solar radiation by five cloud layers as functions of cosine of solar zenith angle. (after Liou, 1976)

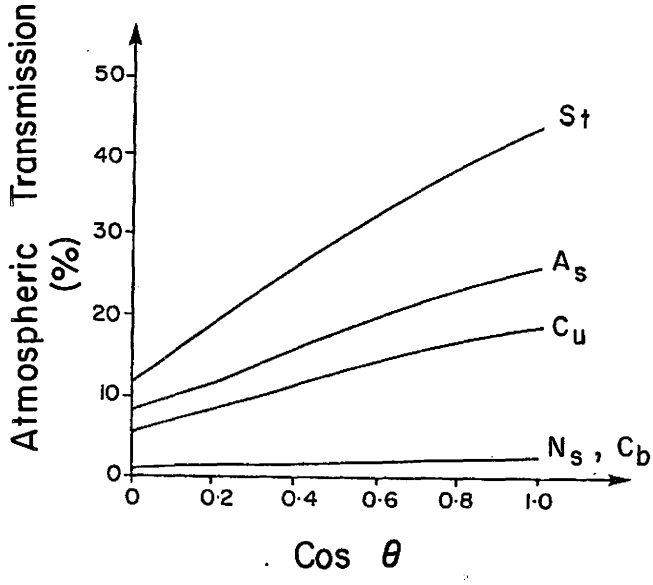

Figure : 18 Transmission of solar radiation at the bottom of five cloudy atmospheres. (after Liou, 1976)

successfully at a number of mid latitude sites (Davies et al., 1975), the need to consider changes in cloud transmission characteristics for Arctic areas were demonstrated by Vowinckel and Orvig (1962). For Arctic coastal areas they noted the following:

1. cloud type transmissivity for Arctic areas is considerably higher than that of lower latitudes due
2. to cloud type transmissivity increases with solar altitude; this increase is small in middle latitudes but considerably higher for Arctic coastal areas,
3. that there is a marked seasonal increase in cloud type transmissivity.

Considering Vowinckel and Orvig's (1962) observations, the large model underestimation of daily observed values occuring from mid May through June (Figure 12) is possibly the result of the seasonal cloud transmissivity change. This would explain the similar shape of the two plots and the build up of low level cloudiness leading to consistent model underestimation of observed values.

Fifthly, the multiply reflected contribution to the surface flux from cloud bases is somewhat dependent on daily changes in surface reflective characteristics. Although no allowance is made for characteristic surface (and cloud base) albedo increases and decreases, with respective low and high zenith angles, daily results are not seriously altered.

CHAPTER FIVE

CONCLUSION

This thesis was directed towards the study of the Davies and Hay (1978) approach for evaluating surface receipts of solar radiation in an Arctic environment. The model was used in the analysis of hourly and daily periods for cloudless and cloudy sky conditions.

From the results, presented in Chapters 4 and 6, important findings can be summarized:

1/ While some seasonal and daily differences undoubtably exist in the atmospheric aerosol content good agreement between measured and calculated direct beam values was obtained using k=0.88. This value of k has been retained by other workers and substantiates its use (Davies et al., Suckling and Hay, 1978). However, it is somewhat smaller than might be expected of a non-urban Arctic environment.

2/ The numerical results presented for cloudless and nearly cloudless conditions show that solar radiation can be calculated with good accuracy ($\pm$10%) for time periods as short as one hour.

3/ For completely overcast conditions, it should be apparent that Haurwitz's (1948) cloud transmission constants serve to underestimate actual cloud transmissions at Resolute. This is of some importance as the Davies and Hay (1978) approach utilized Haurwitz's values.

4/ For small values of cloudiness, it was shown that the model tends to overestimate observed values.

5/ Although averaging daily values over longer time periods did improve model performance a better accounting of Arctic cloud transmission characteristics along with more accurate surface observations is required before the model can be used with confidence.

6/ While seasonal differences were shown to exist in the transmissivity of Arctic clouds (Vowinkel and Orvig, 1962) the variability of a given cloud thickness is likely to be as great as any seasonal differences. Whether such effects can be successfully modelled is a problem for future research.

APPENDIX ONE

NOTATION

Roman Case

$A_{a_o}^{vis}$	absorptivity of ozone in the visible portion of the spectrum
$A_{a_o}^{uv}$	absorptivity of ozone in the ultraviolet portion of the spectrum
B_a	ratio of forward to total scatter
C	cloud amount
D	diffuse radiation
D_A	component of diffuse radiation due to scattering by aerosol
D_R	component of diffuse radition due to Rayleigh scatter
D_S	component of diffuse radiation arising from multiple reflection between the ground surface and the atmosphere
$D\downarrow$	diffuse sky radiation on a horizontal surface
$D\downarrow'$	diffuse sky radiation on a horizontal surface before multiple reflection
I	radiation intensity
$I\downarrow$	direct solar radiation on a horizontal surface
I_o	solar constant
I_{ZT}	instantaneous value of the solar constant (solar constant corrected for sun-earth distance)
K_λ	spectral mass absorption coefficient
$K\downarrow'$	incoming solar radiation on a horizontal surface before multiple reflection
$K\downarrow_o$	total incoming solar radiation under clear sky conditions
$K\downarrow_c$	total incoming solar radiation under cloudy sky conditions before multiple reflection

$K\downarrow_R$	component of the surface solar flux due to cloud base reflection
$K\downarrow$	total incoming solar radiation on a horizontal surface under all sky conditions
LAT	local apparent time
U_{OZ}	ozone in the vertical path length
U_w	water in the vertical path length
W	solid angle
W_o	single scattering albedo
X_1	slant path through ozone
X_2	slant path through water
Z_T	height of the top of the atmosphere
a_o	absorptivity of ozone
a_{wv}	water vapour absorptance
ci	cloud amount in cloud layer i
d	instantaneous sun-earth distance
$\bar{d}$	average sun-earth distance
h	hour angle
k	dust factor constant
m	relative optical air mass
n	total number of cloud layers
r	direction of scattered radiation
r'	direction of incident radiation
t	cloud type transmittance

Greek Case

α_c	cloud base albedo
α_a^*	albedo for aerosol backscattering of surface reflected radiation
α_g	surface albedo
α_R	albedo of the atmosphere for surface reflected radiation
α_R^*	Rayleigh scattering albedo for upwelling radiation
δ	solar declination
θ	solar zenith angle
λ	wavelength
σ_λ	spectral mass scattering coefficient
τ	atmospheric optical depth
τ_a	optical depth for aerosol
τ_o	optical depth for ozone
τ_R	optical depth for Rayleigh scattering
τ_w	optical depth for water vapour
ϕ	latitude
ψ_a	transmittance after extinction by aerosol
ψ_o	transmittance after absorption by ozone
ψ_R	transmittance after Rayleigh scatter
ψ_W	transmittance after absorption by water vapour
$\gamma(\tau, r', r)$	phase function
ζ	air density

REFERENCES

Atmospheric Environment Service: Monthly radiation summary, Ottawa, Information Canada, 1974.

Atmospheric Environment Service: Monthly Bulletin, Canadian Upper Air Data, Downsview, Ontario, 1974.

Atwater, M.A. and P.S. Brown, 1974: Numerical computations of the latitudinal variation of solar radiation for an atmosphere of varying opacity, J.Appl.Meteor., 13, 289-297.

Atwater, M.A. and J.T. Ball, 1976: Comparison of radiation computations using observed and estimated precipitable water. J.Appl.Meteor., 15, 1319-1320.

Braslau, N. and J.V. Dave, 1973: Effect of aerosols on the transfer of solar energy through realistic atmospheres. Part 1: Nonabsorbing aerosols. J.Appl.Meteor., 21, 601-615.

1971: Effect of the transfer of solar energy through realistic model atmospheres. Part 2: Partly-absorbing aerosols. J.Appl.Meteor., 21, 616-619.

Bergsham, R.W. and J.J. Peterson, 1977: Comparison of predicted and observed solar radiation in an urban area. J.Appl.Meteor., 16, 1107-1116.

Catchpole, A.J.W. and D.W. Moodie, 1971: Multiple reflections in Arctic regions. Weather, 26, 157-163.

Davies, J.A., W. Schertzer and M. Nunez, 1975: Estimating global solar radiation. Boundary Layer Meteor., 9, 33-52.

Davies, J.A. and J.B. Idso, 1978: Estimating the surface radiation balance and its components. In Gerber, J.F. and B.J. Banfield (editors), Modification of the Aerial Environment of Plants, ASAE monograph (in press).

Davies, J.A. and J.E. Hay, 1978: Calculation of Solar Radiation Data (in press).

Elterman, L., 1968: UV, visible and IR attenuation for altitudes to 50 km, 1968, Air Force Cambridge Research Laboratories, Environmental Service, Toronto, 45p.

Haurwitz, G., 1948: Insolation in relation to cloud type. J.Meteorol., 5, 110-113.

Hay, J.E., 1971: Computational model for radiative fluxes. Jour.Hydrology (N.Z.), 10, 36-48.

Hay, J.E., 1976: A revised method for determining the direct and diffuse components of the total shortwave radiation. Atmosphere, 14, 278-287.

Hay, J.E., 1978: An Analysis of Solar Radiation Data for Selected Locations in Canada. Atmospheric Environment Service, Toronto (in press).

Houghton, H.G., 1954: On the heat balance of the Northern Hemisphere. J.Meteorol., 11, 1-9.

Hoyt, D.V., 1977: A redetermination of the Rayleigh optical depth and its application to selected solar radiation problems. J.Appl.Meteor., 16, 432-436.

Idso, S.B., 1969: Atmospheric attenuation of solar radiation. J.Atmospheric Sci., 26, 1088-1095.

Idso, S.B., 1970: The transmittance of the atmosphere for solar radiation on individual clear days. J.Appl.Meteor., 9, 239-241.

Kondrat'yev, K.Ya., 1969: Radiation in the Atmosphere, Academic Press, New York, 912p.

Latimer, J.R., 1971: Radiation measurement. International field year for the Great Lakes, Technical manual series, No. 2, 53p.

Latteau, H. and K. Latteau, 1969: Shortwave radiation climatology, Tellus, 21, 208-222.

Lacis, A.A. and J.E. Hansen, 1974: A parameterization for the absorption of solar radiation in the earth's atmosphere. J.Atmos.Sci., 31, 118-133.

Liou, K.N., 1976: On the absorption, reflection and transmission of solar radiation in cloud atmospheres. J.Atm.Sci., 33, 798-805.

List, P.J., 1966: Smithsonian Meteorological Tables. Smithsonian Miscellaneous collection, 114, 527p.

Manobs, Manual of standard procedures for surface weather observing and reporting, Dept. of Transport, Meteorological Branch, Toronto, 1970.

McDonald, J.E., 1960: Direct absorption of solar radiation by atmospheric water vapour, J.Meteor., 17, 319-328.

Monteith, J.L., 1962: Attenuation of solar radiation: a climatological study. Quart.J.Roy.Meteor.Soc., 88, 508-521.

Paltridge, G.W. and C.M.R. Platt, 1976: Radiative Processes in Meteorology and Climatology. Developments in Atmospheric Science, 5. Elsevier, New York, 318p.

Robinson, N., 1966: Solar Radiation. Elsevier, New York, 347p.

Schneider, S.H. and R.E. Dickenson, 1976: Parameterization of fractional cloud amounts in climatic models: the importance of modeling multiple reflections. J.Appl.Meteor., 15, 1050-1056.

Suckling, P.W. and J.E. Hay, 1976: Modelling direct, diffuse and total solar radiation for cloudless days. Atmosphere, 14, 298-304.

Toon, O.B. and J.B. Pollack, 1976: A global average model of atmospheric aerosols for radiative transfer calculations. J.Appl.Meteor., 15, 225-246.

Vowinkel, E. and S. Orvig, 1962: Relation between solar radiation income and cloud type in the Arctic. J.Appl.Meteor., 1, 552-559.

World Meteorological Organization: Ozone data for the World, monthly publication, 1974.

Yamamoto, G., 1962: Direct absorption of solar radiation by atmospheric water vapour, carbon dioxide and molecular oxygen, J.Atmos.Sci., 19, 182-188.